Earth and Space Science

RESEARCH ARTICLE
10.1029/2022EA002584

Key Points:

- AROME/NEMO improves the forecast of tropical cyclone compared to the operational configuration with a 1D ocean mixed layer parameterization
- The improvement mostly comes from quasi-stationary or very slow moving intense cyclones
- The tropical cyclone forecasts are sensitive to the ocean initial conditions

Correspondence to:
S. Malardel,
sylvie.malardel@meteo.fr

Citation:
Corale, L., Malardel, S., Bielli, S., & Bouin, M.-N. (2023). Evaluation of a mesoscale coupled ocean-atmosphere configuration for tropical cyclone forecasting in the South West Indian Ocean basin. *Earth and Space Science*, *10*, e2022EA002584. https://doi.org/10.1029/2022EA002584

Received 19 AUG 2022
Accepted 18 JAN 2023

Author Contributions:
Conceptualization: Laëtitia Corale, Sylvie Malardel, Soline Bielli, Marie-Noëlle Bouin
Supervision: Sylvie Malardel, Soline Bielli, Marie-Noëlle Bouin
Writing – review & editing: Sylvie Malardel, Soline Bielli, Marie-Noëlle Bouin

Evaluation of a Mesoscale Coupled Ocean-Atmosphere Configuration for Tropical Cyclone Forecasting in the South West Indian Ocean Basin

Laëtitia Corale[1], Sylvie Malardel[1], Soline Bielli[1], and Marie-Noëlle Bouin[2,3]

[1]Laboratoire de l'Atmosphère et des Cyclones (LACy), CNRS, Météo-France, Université de La Réunion, Saint-Denis, France, [2]CNRM, Météo-France, CNRS, Université de Toulouse, Toulouse, France, [3]Laboratoire d'Océanographie Physique et Spatiale, CNRS, Ifremer, IRD, IUEM, Université de Brest, Plouzané, France

Abstract The performance in term of tropical cyclone track and intensity prediction of the new coupled ocean-atmosphere system based on the operational atmospheric model AROME-Indian Ocean and the ocean model NEMO is assessed against that of the current operational configuration in the case of seven recent tropical cyclones. Five different configurations of the forecast system are evaluated: two with the coupled system, two with an ocean mixed layer parameterization and one with a constant sea surface temperature. For each ocean-atmosphere coupling option, one is initialized directly with the MERCATOR-Ocean PSY4 product as in the current operational configuration and the other with the ocean state that is cycled in the AROME-NEMO coupled suite since a few days before the cyclone intensification. The results show that the coupling with NEMO generally improves the intensity of cyclones in AROME-IO, reducing the mean intensity bias of the 72 hr forecast of about 10 hPa. However, the impact is especially significant when the TCs encounter a slow propagation phase. For short-term forecasts (less than 36 hr), the presence of a cooling in the initial state that has been triggered by the AROME high-resolution cyclonic winds in a previous coupled forecast already improves the tropical cyclone intensity bias of 2–3 hPa for both coupled or uncoupled configurations.

Plain Language Summary The ocean provides a large part of the energy for the intensification of tropical cyclones through warm sea surface temperature and sea-air heat and moisture exchanges. However, the ocean-atmosphere interactions also trigger processes which cools the sea surface temperature beneath the tropical cyclone and thus generates a negative feedback on the TC intensification. The numerical forecasts of the regional numerical weather prediction model AROME-IO are valuable guidance for the Regional Specialized Meteorological Centre for Tropical Cyclones, La Réunion. The objective of our study is to evaluate the possibility of replacing the current ocean mixed layer parameterization by a more realistic ocean able to represent more complex processes such as the explicit transport by the currents. Overall, we found that the new coupling improves the cyclone intensity in AROME-IO both in terms of bias and standard deviation. These improvements come almost entirely from tropical cyclones that encounter a slow propagation phase. For short-term forecasts, the presence of a cooling that is triggered by AROME high-resolution cyclonic winds in the initial state of the ocean already improves the TC intensity forecast, even when the ocean mixed layer parameterization is used.

1. Introduction

Tropical cyclones (TCs) can be associated with a combination of several hazardous phenomena: storm surges, floods, extreme winds, tornadoes and lightning. They are highly destructive atmospheric phenomena that cause damage to life and infrastructures along tropical coastal areas, particularly in the South West Indian Ocean (SWIO: 30°–90°E, 0°–40°S) tropical islands, where economic vulnerability, fragile infrastructures and confined space make populations highly vulnerable to cyclonic hazards. The SWIO accounts for an average of 12% of annual global cyclone activity with about 10 tropical storms, four of which reach the stage of a tropical cyclone (equivalent CAT2-3 on the US Saffir-Simpson scale, see Leroux et al., 2018). Forecasters of the Regional Specialized Meteorological Centre for Tropical Cyclones (RSMC-Cyclones) of La Réunion are in demand of accurate numerical forecasts of the track and intensity of TC to quickly identify potentially impacted areas and effectively warn communities of the impending danger.

The work carried out in recent years has particularly led to improvements in the forecasting of TC tracks (Courtney et al., 2019; Heming et al., 2019). TC intensity is less predictable as it involves small scales features which are not yet well understood. A number of factors are known as important sources of model uncertainty for the simulation of TC intensification. The horizontal resolution of the models is a key factor for a fine description of both the small scale processes such as convective updrafts or density currents but also the very strong gradients that characterize the TC structure. Atmospheric cloud resolving model at kilometric resolutions are necessary to explicitly represent the interaction between the convective towers in the TC wall and the primary and secondary circulations of the TC. The numerical representation of the TC structure and intensity are therefore sensitive to the quality and complexity of the cloud microphysics scheme in the atmospheric model (T. Hoarau et al., 2018). As TC are mostly fueled by the ocean, the parametrization of the heat, momentum and water vapor exchanges between the atmosphere and the ocean is an other key factor for the modeling of TCs. For strong wind, the uncertainty of the ocean-atmosphere flux parametrization is large mainly because the direct or indirect flux observations for winds above 25 m/s which could be used to improve the flux schemes are very rare. New parametrizations are currently developed and tested in order to improve the current bulk schemes. The explicit coupling between the flux formulation and the output of a wave model is one of the areas for improvement for schemes whose formulation of the exchange coefficient is a direct function of the roughness length (Bidlot, 2022; Janssen et al., 2002; Moon et al., 2004). The effect of sea spray is an other factor which can be explicitly taken into account in the flux scheme and is the subject of active research (Andreas et al., 2015; Shpund et al., 2019).

The ocean-atmosphere (OA) feedback in intense TC condition has also been recognized as one of the key elements of the progress for TC intensity forecasting (Feng et al., 2019; Mogensen et al., 2017; Vellinga et al., 2020; Yablonsky, 2016). This study explores this avenue of improvement for the numerical prediction of tropical cyclones in the SWIO basin which is considered as the cyclonic basin with the highest importance of OA interactions (Vialard et al., 2008) because of the unique thermocline structure in the Seychelles-Chagos thermocline ridge area (55°–70°E, 5°–15°S) (Hermes & Reason, 2009). Indeed, this zone which is characterized by a near-surface thermocline and a shallow mixed layer, where sea surface temperature (SST) values can reach 28.5–30°C during the heart of the SWIO cyclone season (January and February) is very active in terms of TC cyclogenesis.

The ocean provides a large part of energy for the intensification and persistence of TCs through warm SST and air-sea heat and moisture fluxes. However, the OA interactions also trigger processes which cools the SST beneath the TC and thus generates a negative feedback on the TC intensification (Srinivas et al., 2016). The sea surface cooling is mainly governed by three different processes:

- a loss of energy associated to the heat and evaporation fluxes toward the atmosphere,
- the vertical turbulent mixing in the upper ocean which cools the ocean mixed layer (OML) by mixing the warm water above the thermocline with the colder water below. This process tends to deepen the OML.
- The vertical transport of deeper cold water by upwelling generated by Ekman pumping (Bender et al., 1993; Black, 1983; Price, 1981). In the vicinity of a TC, the winds combined to the TC displacement generate divergent currents at the surface which then trigger an upwelling of cold deep water across the thermocline toward the surface.

The respective part of these different processes depend largely on the cyclone intensity and ocean preconditioning (Vincent et al., 2012). According to Vincent et al. (2012) and Jullien et al. (2012), the surface heat fluxes are dominant for weak to medium intensity cyclones, while the turbulent mixing accounts for 30%–50% of the surface cooling for weaker cyclones but for more than 80% for the most intense. The effect of the upwelling of colder water increases with the cyclone intensity to reach 20% for the most intense cyclones. Especially, its effect is crucial to explain the asymmetry of the cold wake with respect to the cyclone direction. The strength of the negative feedback between the TC and the ocean and the cooling of the surface waters is influenced by different factors such as the translation speed and the depth of the OML (Schade & Emanuel, 1999). Using a simple coupled model, Schade and Emanuel (1999) suggest a range of 10%–60% decrease in storm intensity if the storm translation speed is reduced in their academic test cases. Similarly, Yablonsky and Ginis (2009) demonstrate the importance of a three-dimensional (3D) ocean model for resolving SST cooling when simulating a TC moving at a speed of 5 m s^{-1} and even more critical for slower systems. The depth of the OML and the oceanic stratification also plays an important role in the O-A feedback as shown in the following studies (Jullien et al., 2014; Lin et al., 2008; Schade & Emanuel, 1999). The amount of mixing which is necessary to modify the SST in a deep

OML is much larger than in a shallow OML. The SST cools then more rapidly in shallow OMLs and the negative retroaction between the TC winds and the cooling at the surface on the TC intensification is more effective. Other subsurface ocean features such as the thermocline stratification due to salt layers for instance or fine scales structures associated with fronts and eddies also have the potential to affect storm intensity. For example, the deeper mixed layer of warm-core eddies is known to favor TC intensification (Bao et al., 2000; Chang & Anthes, 1978). Coastal effects such as the horizontal advection of warm water by coastal currents may also contribute to the fluctuation in intensity of a TC (see e.g., Castillo et al., 2022).

The mesoscale numerical weather prediction model "Applications de la Recherche à l'Opérationnel à Méso-Echelle - Indian Ocean" (AROME-IO) provides 4 times a day a 48 hr forecast for a large SWIO domain. During the SWIO TC season, AROME-IO products provide valuable information on TC intensity to the RSMC-Cyclones of La Réunion. In its original version, the SST was kept constant along the forecast. In such a case where the coupling between the atmosphere and the ocean is disable, the ocean acts as a non limited energy source for the TCs which then tend to be overactive. In its current operational version, AROME-IO is coupled every 5 min to a one-dimensional (1D) parameterization of the OML that takes into account the rapid change of the SST due to the OA heat exchanges and the turbulent mixing of the OML that is triggered by cyclonic winds. The 1D parameterization of the OML is able to reproduce the cooling of the SST underneath the TCs due to the energy and momentum exchanges at the surface and the turbulent mixing. However, its reduced physics does not allow the explicit horizontal and vertical transport and the acceleration by the pressure gradient force. The cooling by the upwelling triggered by Ekman pumping is then not accounted for by the OML parametrization. The numerical simulation of such a process driven by the explicit advection of the oceanic currents needs a 3D ocean model (Mogensen et al., 2017; Yablonsky & Ginis, 2009). Numerous studies have indeed shown the benefit of modeling the upwelling effect in a 3D ocean model for TC forecasting (Bender et al., 2007; Bielli et al., 2021; Ginis, 2002; Jullien et al., 2014; Mogensen et al., 2017; Yablonsky & Ginis, 2009).

The main objective of this study is then to analyze the impact of replacing the current 1D OML parameterization by a fully 3D coupling with the ocean model NEMO (The Nucleus for European Model of the Ocean, Madec et al., 2019) in the operational high resolution mesoscale cloud model AROME-IO (Bousquet et al., 2020; Seity et al., 2011) used by the RSMC of La Réunion. This paper does not aim at analyzing in detail the OA processes in TC case studies as the current knowledge of the main OA interaction mechanisms in a TC is already quite advanced and well documented. It rather focuses on the impact of changing the representation of the ocean component in the forecast system in term of TC forecast. The other aspect which is explored in this study is the design of the ocean initial condition in a coupled forecast suite. Currently, the atmospheric and oceanic initial conditions of most operational coupled system as the Integrated Forecast System (IFS) of the European Centre for Medium-Range Weather Forecasts (ECMWF) are produced by independent data assimilation systems. The lack of balance in the boundary layer of both the atmosphere and the ocean may then create an initial choc which perturbs the short range of the forecast. A coupled data assimilation is the solution to create balanced atmospheric and ocean initial states and it is an active domain of research with still many scientific and technical problems to be solved (Browne et al., 2019; Penny et al., 2017). For a regional model without data assimilation such as AROME-OI, the initialization of the atmosphere is based on a lower resolution global analysis. However, building up the small scales in the higher resolution model is not instantaneous and a warm-up algorithm is necessary to accelerate the resolution adjustment in the regional model (see Section 2.1). In the case of an OA coupled regional model, the initialization of the ocean is an open question that we have started to address in this study.

Thus, five different configurations of the AROME-IO modeling system have been set up for this study in order to test both the importance of the complexity of the ocean representation (1D vs. 3D) and the impact of the choice of the oceanic initial condition in a forecast suite. Numerical simulations have been performed for a selection of seven TCs that developed over the SWIO basin during the 2018–2019 and 2019–2020 cyclone seasons. This large set of forecasts has then been analyzed in order to assess the model configuration in terms of track, intensity and structure of the TCs.

The plan of the paper is detailed as follows. Section 2 presents the forecast system AROME-IO, the experimental coupled system AROME-IO/NEMO and the description of the setups of the different numerical simulations performed in this study. The results of the simulations are analyzed in Section 3. First, the statistical impact of the 3D OA coupling and the choice of initial conditions is assessed with scores (bias and standard deviation) against the Best-Track (BT) data for all the TC simulations, then separately for TCs with slow or fast translation speed.

Second, we further analyze the results of the simulations with three test cases: one in the slow propagation speed category (TC Gelena, February 2019), one in the fast propagation speed category (TC Belna, December 2019) and one for which buoy measurements enable a direct comparison of the modeled SST cooling with observations (TC Batsirai which encounters a phase of slow propagation at the beginning of February 2022). Conclusions and perspectives are given in Section 4.

2. Tools, Methods, and Data

In this section, we give a short description of the numerical systems used for this study. We then describe the five different types of simulations which have been performed for 31 initial dates and which are analyzed in Section 3.

2.1. The AROME-IO Operational System

AROME-IO (see Faure et al. (2020) and Bousquet et al. (2020) for more details) is an overseas version of the AROME-France model, which is the operational convection permitting, limited area, numerical weather prediction model used at Météo-France since 2008. Since 2016, AROME-IO produces 48 hr forecasts (78 hr on demand) 4 times a day over an area of 3,000 km by 1,400 km (30°−70°E, 7°–22°S) encompassing most islands of the SWIO. Its horizontal resolution is 2.5 km and the time step is 60 s. In the vertical, 90 levels are distributed between the surface (first level at 5 m and 34 levels within the first 2 km) and 10 hPa. The AROME-IO operational configuration is initialized from the High RESolution Integrated Forecasting System (HRES IFS) European Centre for Medium-Range Weather Forecasts (ECMWF) model (currently about 9 km horizontal resolution), which also provides the lateral boundary conditions at the frequency of 1 hr. An IAU (Incremental Analysis Update; Bloom et al., 1996) initialization scheme is used to build the small-scale features which are modeled with the resolution of AROME but not with the resolution of the IFS. Such a warmup procedure reduces the initialization choc at initial time t_0. The IAU algorithm combines the ECMWF larger scale analysis increments (temperature, wind, humidity, and surface pressure at 9 km resolution) valid at t_0 with a 6 hr AROME-IO forecast which had directly been initialized by the interpolation on the 2.5 km AROME grid of the ECMWF analysis at $(t_0 - 6)$ hours.

The atmosphere-sea surface exchanges are represented by the Exchange Coefficient Unified Multi-campaign Experiments (ECUME) parameterization (Belamari, 2005; Weill et al., 2003) which is part of the EXternalized SURface platform SURFEX (Voldoire et al., 2017). Moreover, AROME-IO is coupled every 300 s to a 1D OML model (Gaspar et al., 1990; Lebeaupin Brossier et al., 2009) in order to better take into account the feedback between the atmosphere and the ocean in cyclonic conditions. In the current configuration, the OML prognostic parameters (salinity, temperature and currents) are initialized from the first 26 levels (depth of about 180 m) of the MERCATOR-Ocean global product PSY4 (Lellouche et al., 2018) which are available every 6 hr (1 hr means).

The 1D OML parameterization is built on a partial representation of the ocean processes which are triggered by winds. The advection and pressure gradient terms are neglected in the system of dynamic and thermodynamic equations. The water columns are therefore independent of each other. As a consequence, there is no vertical velocity generated by the divergence or convergence of currents and thus no upwelling and downwelling. The OML model reproduces only the turbulent exchanges between the ocean and the atmosphere and the turbulent mixing thanks to a 1.5 order turbulent scheme directly adapted for the ocean from the Turbulent Kinetic Energy (TKE) scheme used in AROME (Bougeault & Lacarrere, 1989).

In a limited area model, the TCs track are mostly driven by the large scale environment of the TCs. Thus, in AROME, they usually follow the IFS track. The score of the short term AROME forecast in term of TC position error is then very similar to the one of the HRES IFS (Figure 1a). The mesoscale model AROME significantly improves the short term forecast of TC intensification compared to the HRES-IFS model which regularly underestimates TC intensities (Figures 1b and 1c). AROME shows however a general tendency to overestimate the TC intensification of the most intense systems (about 3 hPa and 4 $m.s^{-1}$ after 42 hr of forecast). It is therefore hypothesized that a better representation of the interaction between the cyclonic circulation and the oceanic surface in the OA coupled model will reduce the TC intensification in the model thanks to the generation of a cold upwelling underneath. The results presented in the following subsections demonstrate that it actually contributes to the reduction of the positive bias error in intensity, even if other factors such as uncertainties in the parameterization of the surface fluxes and in the microphysics scheme (see also the discussion in the conclusion) may still explain AROME overactivity.

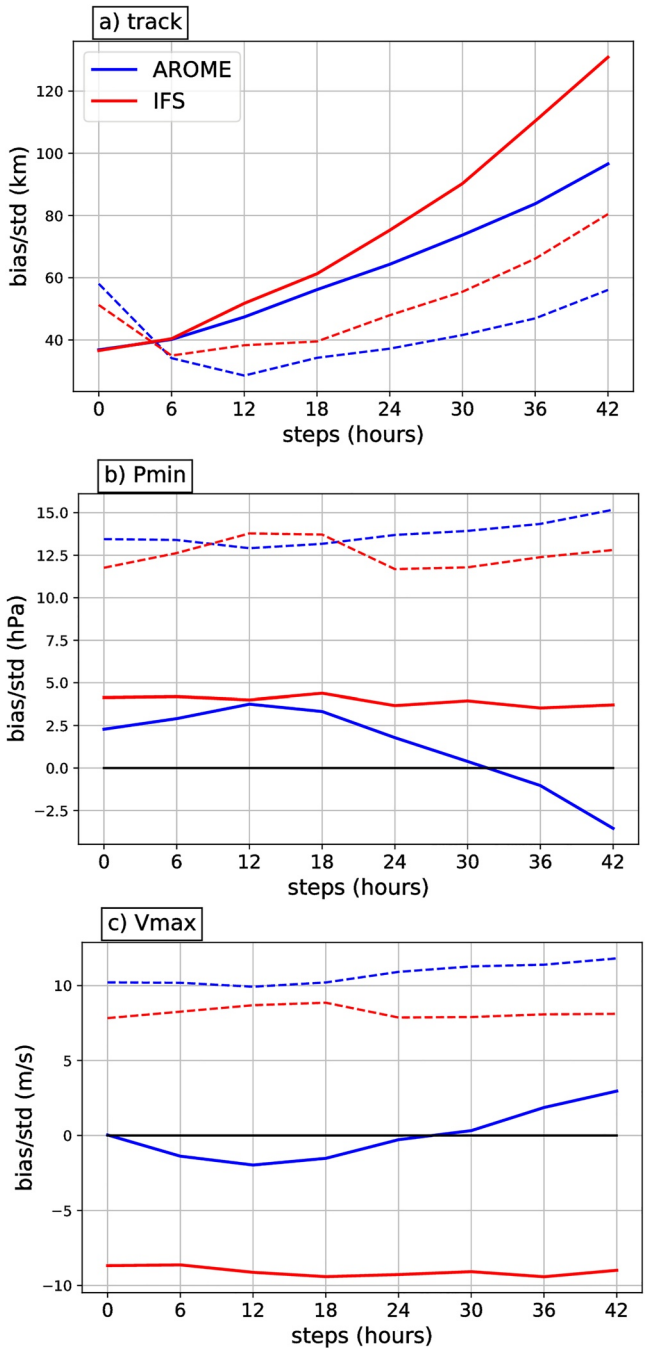

Figure 1. Bias (solid lines) and standard deviation (dashed lines) for (a) the TC center position, (b) the minimum of pressure at the center of the TC and (c) maximal 10-m wind in the TC wall for IFS (red) and AROME-IO (blue) against the BT for all TCs of the 2018–2019 and 2019–2020 in the AROME-IO domain.

2.2. The AROME-NEMO Coupled System

The experimental coupled system AROME-NEMO which has been implemented in the context of this work combines the AROME-IO atmospheric model (Faure et al., 2020) and a regional version of the NEMO ocean model (Madec et al., 2019). The coupling between these two components is controlled by the OASIS3-MCT coupler (Craig et al., 2017).

NEMO is the European modeling framework for oceanographic research, operational oceanography, seasonal forecasting and climate studies. This study uses the version 3.6 of the code with the same ORCA grid (tripolar grid with variable horizontal resolution; Madec & Imbard, 1996) at the horizontal resolution of a 1/12° (about 9 km in the SWIO region) and the same 50 unevenly spaced vertical levels as the PSY4 global operational products of MERCATOR-Ocean. The NEMO domain covers the whole oceanic part of AROME-IO. The bathymetry is based on the ETOPO1 database (Amante & Eakins, 2009). The vertical mixing is a TKE closure scheme based on the work of Gaspar et al. (1990) (like the 1D OML used in this study), but with important modifications introduced by Madec et al. (1998) in the implementation and formulation of the mixing length scale. In the current configuration, the barometric effect on the sea surface height and the tidal forcing are switched off (default configuration).

In the configuration used in this study, NEMO provides to OASIS the 1 hr mean SST with a coupling frequency of 1 hr which is commonly used for the a 1/12° resolution in the NEMO community. The SST is used to compute the air-sea fluxes at each subsequent atmospheric time step. The effect of surface currents on surface fluxes and atmospheric low-level flow (Lemarié, 2015; Renault et al., 2019) is not considered yet in this study as the modification of the turbulent scheme in AROME which is necessary to account for the relative motion of the air with respect to the current was not yet available when this work started. The 1 hr mean solar and net heat fluxes and the components of the horizontal wind stress and atmospheric freshwater are returned to OASIS by SURFEX and then sent to NEMO with a 1 hr coupling frequency (Figure 2). The corresponding equations and the description of the coupling strategy are detailed in Voldoire et al. (2017).

On the Météo-France supercomputers, the extra computing cost of the oceanic model at a 1/12° resolution and a coupling frequency of 1 hr is negligible compared to the cost of the atmospheric model. For example, the current prototype runs on 480 processors for AROME-IO against only 32 processors for NEMO. So, the computing cost would not be a limitation for a potential operational use of the coupled system. Note also that the cost of the OML scheme is negligible, less than the 5% variability of the computer cost estimations which fluctuates with the activity of the supercomputer.

2.3. Description of the Numerical Configuration Set-Ups

The main objective of this study is to evaluate the sensitivity of the AROME-IO TC forecasts skill to the numerical representation of the ocean underneath. Three degrees of complexity of this representation are compared with each other in this study:

- constant SST along the forecast,
- evolution of the first layer of the ocean estimated by a 1D parametrization of the OML. In this configuration, both the SST and the first 180 m of the ocean evolves in time and interact with the atmosphere above thanks to the surface fluxes. In this case, the only mixing process in the OML is the subgrid turbulent mixing which

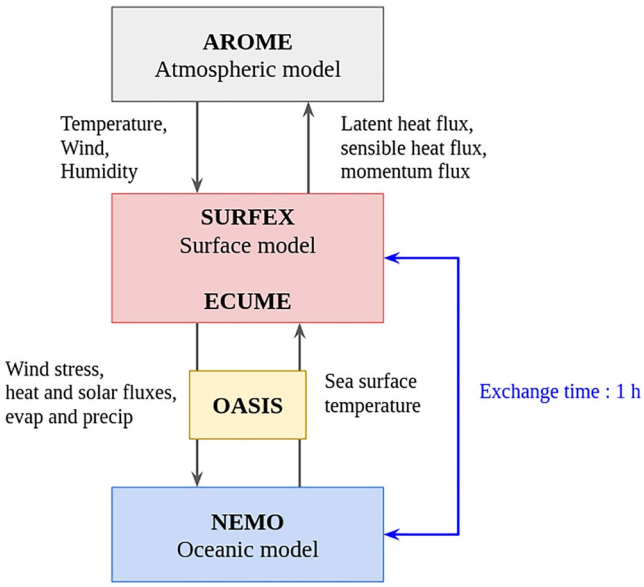

Figure 2. Schematic diagram of the coupling between AROME and NEMO via SURFEX and OASIS.

is parametrized by a prognostic TKE scheme (Gaspar et al., 1990). There is no horizontal and vertical advection by the currents and the effect of pressure gradient force on the current acceleration is neglected.

- evolution of the ocean state computed by the 3D ocean model NEMO. As in the previous case, the ocean interacts with the atmosphere through the surface heat and momentum fluxes. But in this case, the transport generated by the currents and the retroaction of the mass redistribution on the current acceleration (pressure gradient force) is taken into account by the 3D ocean model. The SST is still changing because of turbulent mixing but also because of the horizontal advection and the vertical advection (upwelling/downwelling) by the currents which are associated with the 3D oceanic circulations modeled by NEMO.

As an other objective of this work is to advice on the design of a future coupled operational system, two different solutions for the initial oceanic state have been used for both the OML and the coupled simulations.

In a first solution, the ocean model is directly initialized with the PSY4 products provided by MERCATOR-Ocean. Such a solution is currently used in operation to initialize the OML at the beginning of each new forecast.

As the state of the ocean in the PSY4 global products is quite "smooth," the SST cooling and the upwelling generated by TCs are much weaker than in the AROME-NEMO coupled configuration (see discussion in Section 3). Test simulations (not shown) with a forced configuration of NEMO using IFS or AROME winds showed that the main reason explaining the difference of SST cooling induced by TC circulations between PSY4 and AROME-NEMO is the strength of the winds forcing the ocean. As pointed out by several recent studies, strong winds in the ECMWF IFS- WAve Model (WAM) configuration are generally underestimated (Haiden et al., 2018; Magnusson et al., 2019; Pineau-Guillou et al., 2018) whereas the wind from the current AROME-IO operational system are much closer to the wind estimated by the BT (Bousquet et al., 2020; see also Figure 1). We then decided to set up a second solution in which the ocean model is initialized by an ocean state resulting from a previous AROME-NEMO coupled run. Cycling the ocean without any relaxation toward observation is a solution which can be used only for a few days in a row. But, in the context of the TCs simulations conducted for this study, we think that this second solution emulates a forecast suite where the ocean would be initialized by an ocean analysis forced with the AROME winds instead of the IFS winds or by a combination between a smooth ocean analysis and an oceanic state issued from a previous coupled AROME-NEMO run. In practice, the coupled simulations start about a week before the TC enters the AROME domain. The very first coupled simulation is initialized with PSY4, then, 24 hr later, the next NEMO simulation starts from the state of the ocean of the 24 hr forecast of the previous coupled simulation. In order to test the impact of the initial state of the ocean only in the current operational configuration, the "cycled" state of the ocean is also used to initialized the OML in an other series of simulations.

In total, five different configurations have been implemented (Table 1):

- **SST cste** the SST field is initialized with the PSY4 ocean state and it is kept constant in the forecast. This configuration has been used in AROME-IO between 2016 and the end of 2017, prior to the implementation of the OML parameterization. It is also still the configuration of AROME-France.
- **OMLpsy4** The 1D parametrization of the OML is switched on in SURFEX and it is initialized by the PSY4 products provided by MERCATOR-Ocean. This is the configuration of the current operational system (see Section 2.1).

Table 1
Summary of the Five Simulation Types Which Are Analyzed in This Work

	SST cst	OMLpsy4	OMLcyO	CPLpsy4	CPLcyO
Ocean configuration	None	1D OML	1D OML	3D ocean	3D ocean
Initial ocean state	PSY4	PSY4	Cycled ocean	PSY4	Cycled ocean

Table 2
Name and Characteristics of the Selected TCs

	SWIO classification	Maximum average wind (m s^{-1})	US Saffir-Simpson scale
Gelena	Intense tropical cyclone	57	CAT3
Idai	Intense tropical cyclone	49	CAT2
Kenneth	Intense tropical cyclone	57	CAT3
Belna	Tropical cyclone	42	CAT1
Calvinia	Tropical cyclone	33	CAT1
Diane	Moderate tropical storm	21	Tropical storm
Herold	Intense tropical cyclone	46	CAT2
Batsirai	Intense tropical cyclone	57	CAT3

Note. The maximum average wind is based on BT data.

- **OMLcyO** The 1D parametrization of the OML is switched on in SURFEX. The OML is initialized with an ocean state from the previous AROME-NEMO coupled run (see configuration CPLcyo below).
- **CPLpsy4** AROME-IO is coupled with NEMO (the OML scheme is switched off). NEMO is initialized with the PSY4 products provided by MERCATOR-Ocean.
- **CPLcyO** AROME-IO is coupled with NEMO (the OML scheme is switched off). NEMO is initialized with an ocean state from the previous AROME-NEMO coupled run.

In order to focus on the sensitivity to the ocean initial conditions, all five configurations start from the same atmospheric state which is taken from the operational AROME-IO model. This means that the 6 hr warmup is done with the OMLpsy4 configuration and the result is used as the initial condition of all five configurations. A few tests have been done with the same configuration both in the warmup and the 72 hr forecast. But, the spread (from 0.5 m s^{-1} on average to 5 m s^{-1} in the most extreme cases such as TC Gelena) in the TC characteristics after the warmup made the comparison between the different oceanic configuration difficult, hence our choice to start all configurations with the same atmospheric state for this study.

For each configuration, we have then set up a "light" NWP suite with only one 72 hr forecast per day, at 00 UTC. The CPLcyO suites start a few day before a TC enters the AROME-IO domain. The five suites have been run for seven different TCs that have been selected for various tracks and intensities (see Table 2) and with reasonable track prediction. The tracks of the seven cyclones are shown in Figure 3 and their intensity is indicated by color dots corresponding to the five categories used in the SWIO basin: Tropical Depression (TD, $13 < V_{max} < 16$ m s^{-1}), Moderate Tropical Storm (MTS, $17 < V_{max} < 24$ m s^{-1}), Strong Tropical Storm (STS, $25 < V_{max} < 32$ m s^{-1}), Tropical Cyclone (TC, $33 < V_{max} < 43$ m s^{-1}), and Intense Tropical Cyclone (ITC, $V_{max} > 44$ m s^{-1}) where V_{max} is the 10 min averaged maximum wind speed.

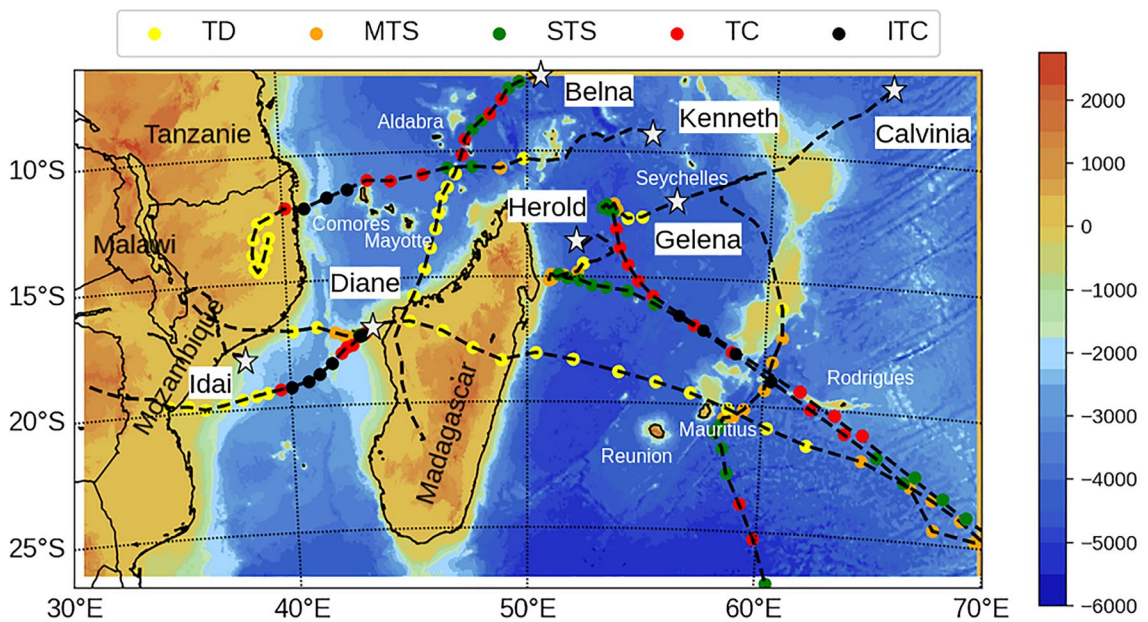

Figure 3. Orography and bathymetry (shading, in m) of the AROME-IO/NEMO coupled system. Track and intensity of Gelena, Idai, Kenneth, Belna, Calvinia, Diane, and Herold as estimated by the RSMC of La Reunion. The SWIO intensity classification: Tropical Depression (TD, $13 < V_{max} < 16$ m s^{-1}), Moderate Tropical Storm (MTS, $17 < V_{max} < 24$ m s^{-1}), Strong Tropical Storm (STS, $25 < V_{max} < 32$ m s^{-1}), Tropical Cyclone (TC, $33 < V_{max} < 43$ m s^{-1}), and Intense Tropical Cyclone (ITC, $V_{max} > 44$ m s^{-1}) where V_{max} is the 10 min averaged maximum wind speed. (add island names).

Table 3
List of the 31 Forecasts Used for the Statistics

Gelena	Idai	Kenneth	Belna	Calvinia	Diane	Herold
05/02/2019	**09/03/2019**	23/04/2019	06/12/2019	26/12/2019	23/01/2020	13/03/2020
06/02/2019	**10/03/2019**		07/12/2019	27/12/2019	24/01/2020	**14/03/2020**
07/02/2019	**11/03/2019**		08/12/2019	28/12/2019	25/01/2020	**15/03/2020**
08/02/2019	12/03/2019		09/12/19	29/12/2019		**16/03/2020**
09/02/2019	13/03/2019			**30/12/2019**		17/03/2020
10/02/2019	14/03/2019					18/03/2020

Note. Dates in bold include a period when the TC is quasi-stationary (slow moving): translation speed $\leq$2 m s^{-1} for at least 12 hr.

For each suite, 31 forecasts have been produced sampling seven different TCs with one to six 72 hr forecasts each (see Table 3). Large initial intensity errors are sometimes inherited from the IFS analysis despite the 6 hr warmup. In such cases, we focus on the differences between the five configurations rather than on a comparison with the BT.

2.4. Best-Track Data in the SWIO

Tropical cyclone forecasters at RSMC-La Réunion do not regularly benefit from in-situ measurements within tropical cyclones as it is the case in the North Atlantic or in the Northwest Pacific. As a result of the lack of aircraft reconnaissance and the fact that conventional data are very sparse in the RSMC-La Réunion area of responsibility, the monitoring of tropical systems essentially relies on satellite imagery, except when these systems are within the scope of La Réunion or Mauritius radars. Thus, the satellite-based DVORAK technique (Dvorak, 1975, 1984) which has been used since 1982 at the RSMC-La Réunion remains the main tool available to analyze storms intensity and structure. Since the late 1990s, forecasters have also been using information from microwave imagers/sounders and the associated objective guidance (ADT, AMSU, SATCON) along with scatterometer data such as the currently operational ASCAT and SCATSAT, to refine intensity estimation. However, scatterometer wind measurements are limited to about 25 m/s. Recently, the experimental use in near-real time of SAR wind data allowed a direct estimation of very strong TC winds (50–70 m/s) at a resolution of about 3 km (Duong et al., 2021).

At the end of each tropical cyclone season, the RSMC re-examines and possibly updates the objective analyses which had been established in real time using new information which were not available during the initial TC monitoring. The RSMC "best-tracks" (later referred to as BT) digital data are then mailed to the National Climatic Data Center (Asheville-USA) for integration within the global IBTrACS database and to some other interested Weather Centers. The access to this database is also possible via the RSMC website. The BT data provide the minimum of pressure and the maximum wind (10 min average) for each TC in the SWIO, every 6 h during its life cycle. In this study, these data are considered as the best available reference in term of macroscopic description of TC intensity in the SWIO. They are compared to the minimum of pressure and the maximum wind which are computed by a tracking algorithm from the outputs of the numerical simulations.

3. Results

The aim of this section is to evaluate the coupled OA configuration and estimate its viability in an operational forecasting context. The first part of the section is a statistical analysis of the 31 runs which have been produced for each of the five model configurations. The second part of the section focuses on two particular cyclone cases which have been chosen according to their translation speed, the oceanic conditions at the beginning of the simulation and their impact on the ocean.

Compared to the Atlantic or North Pacific basin, there is a scarcity of both atmospheric and oceanic observational data in the SWIO basin (Bousquet et al., 2021). We then mainly use the BT data for the evaluation of the track and intensity of the TC. When available, we the SAR (Synthetic Aperture Radar) observations for the evaluation

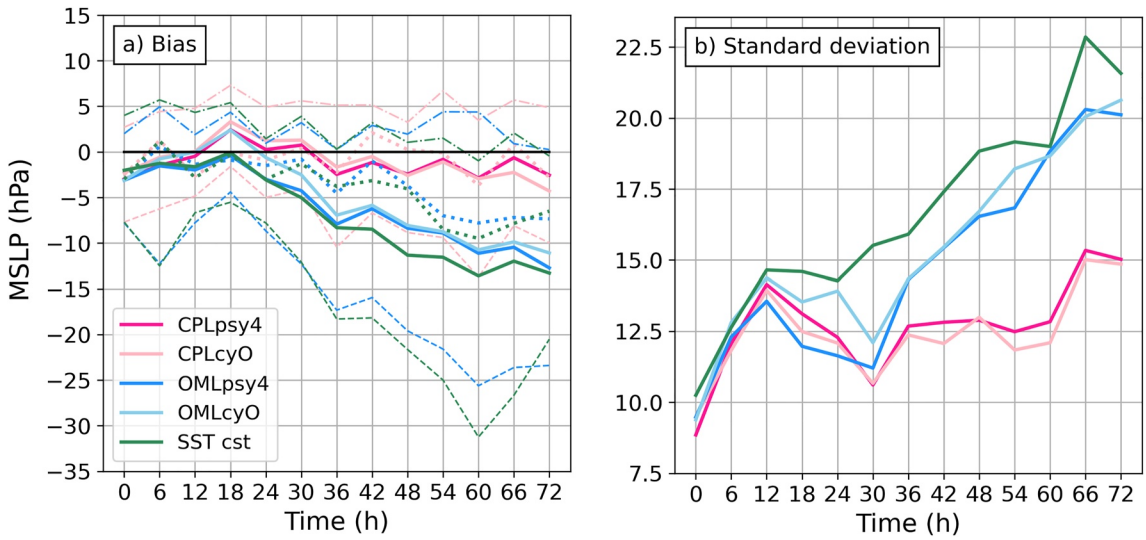

Figure 4. (a) Bias (solid line) and (b) standard deviation for P_{min} (hPa) derived from CPLpsy4 (dark pink), CPLcyO (light pink), OMLpsy4 (dark blue), OMLcyO (light blue) and SST constant (green) simulations against the BT. On panel (a), the dotted lines, dashed lines and alternating lines represent respectively median, first quartile and third quartile for CPLcyO, OMLpsy4 and SST cst. For readability, the quartile for CPLpsy4 (similar to CPLcyO) and OMLcyO (similar to OMLpsy4) are not plotted. The statistics are based on 31 runs (corresponding to the initial times listed in Table 3) for seven different TCs.

of stronger surface winds (Mouche et al., 2017). Ocean sensors such as ARGO profilers or moored buoys are rare and often far from the cyclonic area of interest. SST measurements from Earth observation satellites are usually very incomplete because of the heavy cloud cover in TC condition. It is therefore quite difficult to provide an accurate validation of the temperature predictions of ocean models in cyclonic conditions. A comparison between the modeled oceanic state and observation from a drifting buoy has been exceptionally possible in the case of TC Batsirai. The result of this validation is shown in Section 3.4.

3.1. Scores Against the Best-Track

The TCs are tracked in all 31 forecasts of each of the five configurations (Tables 1 and 3).

The TCs minimum mean sea level pressure (P_{min}) and V_{max} are then compared to the BT data which are considered as the reference in this study. The P_{min} bias and standard deviation against the BT are shown in Figure 4. Conclusions are very similar for V_{max} (not shown).

Both constant SST runs (green curves) and OML runs (blue curves) overestimate the intensity of the TCs with a mean bias (solid line) of more than 10 hPa after 72 hr of simulation. The OML simulations show however a slightly reduced bias (about 3 hPa less) between +48 and +60 hr of simulation and a better standard deviation than the constant SST runs. The first and third quartiles plotted on Figure 4a show that the error distribution of the non coupled runs is skewed with larger negative errors (until −30 hPa for the constant SST configuration at +60 hr) than positive errors (less than +5 hPa for all non coupled configurations). As a consequence of the skewness, the median (dotted line) is 2–5 hPa closer to the BT than the mean. As expected, the coupling with a 3D ocean significantly reduces the mean bias which remains in the range −2 hPa to 2 hPa. The error distribution is less skewed than with the non coupled simulations which indicates that there are less extreme intensifications in the coupled experiments. The standard deviation after 30 hr of simulation is also improved in the 3D coupled forecasts. The TCs characteristics in the OMLcyO simulations remain close to the ones in the CPLcyO runs for about 24/36 hr but then, the scores of the OMLcyO runs quickly degrade as the state of the ocean modeled by the OML parametrization moves away from the true state. After 72 hr of simulation, it reach the same bias and standard deviation as the runs with the operational configuration OMLpsy4.

As we expect the slow or quasi-stationary TCs to be the most sensitive to the 3D coupling with NEMO, we have split the original 31 dates into two groups. A first group, later referred to as slow TCs, contains runs for which the translation speed of the TC is less than or equal to 2 m s^{-1} for at least 12 hr (10 runs in Table 3). The remaining

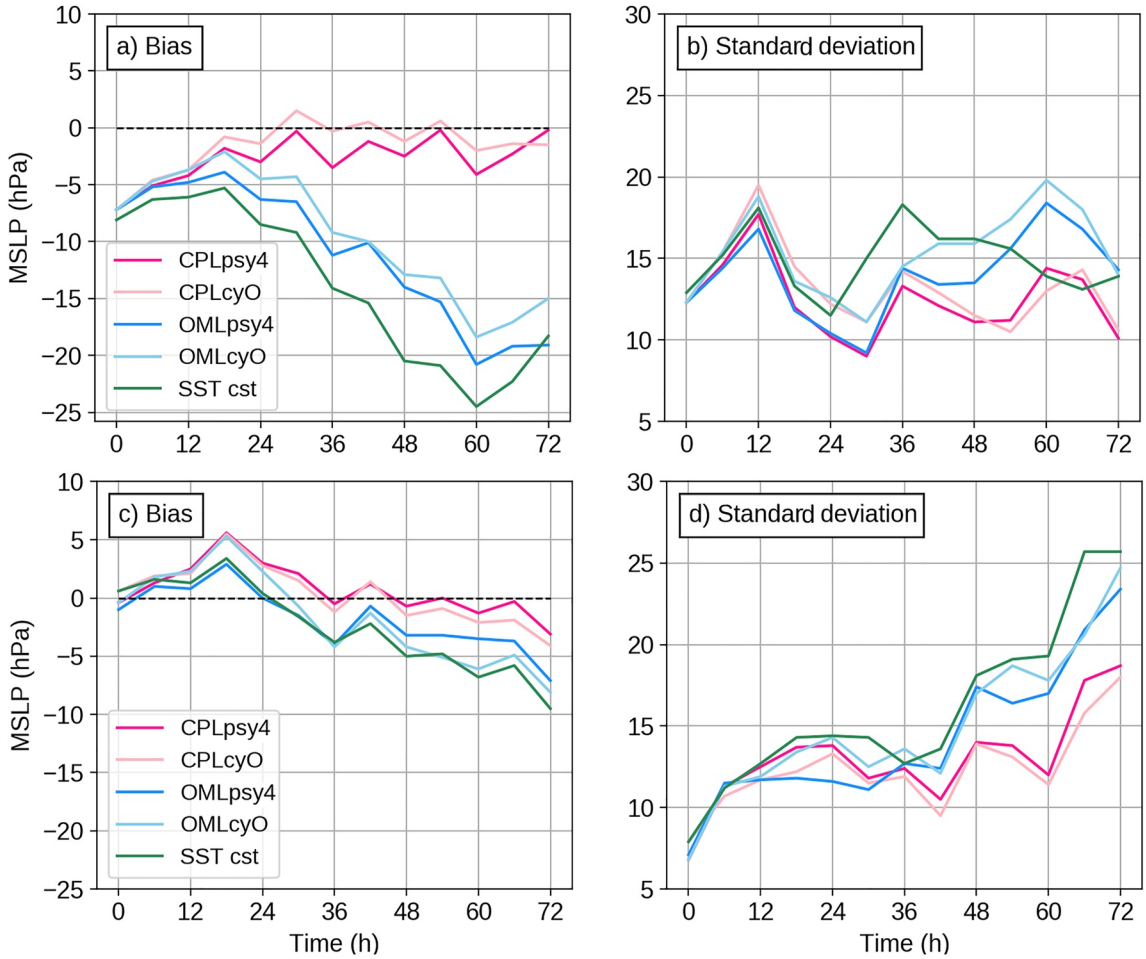

Figure 5. (a–c) Bias and (b–d) standard deviation for P_{min} (hPa) derived from CPLpsy4 (dark pink), CPLcyO (light pink), OMLpsy4 (dark blue), OMLcyO (light blue) and SST constant (green) simulations against the BT for (a and b) slow-moving storms (TC velocity $\leq$2 m s^{-1} for a minimum of 12 hr) and (c and d) fast-moving storms.

runs (21 runs) form a second group of regular or fast moving TCs. For simplicity, we will later referred to Group 2 as "fast" TCs. The statistics have been recomputed for each group (Figure 5).

Figure 5 shows the P_{min} bias (left) and standard deviation (right) against the BT data for the slow (top) and fast (bottom) groups. It clearly confirms that the 3D coupling between AROME and NEMO really matters for the intensity of the slow-moving storms with the bias of the OML simulations 20 hPa larger after 72 hr than the one in the CPL simulations. The impact of the 3D coupling is much smaller for the fast-moving TCs, with a tendency for the coupled runs, but also the OML run starting from the cycled ocean state to weakly underestimate the intensity of the TCs in the first 24 hr. The behavior of the model at the beginning of these simulations may be improved in a configuration where the 6 hr IAU warmup uses the same configuration as the forecast. It is not the case here as all runs starts with the same initial atmospheric condition that is the result of the IAU warmup of the operational configuration (OMLpsy4). The coupled runs and OMLcyO may suffer from a spin-up period as the atmospheric boundary layer and the ocean adjust to each other and thus delay the intensification. More work would be needed to improved the consistency between the atmospheric and oceanic initial conditions in order to palliate the lack of OA coupled data assimilation, but this is beyond the scope of the present study.

In summary, the scores against the BT suggest that:

- The 3D coupling statistically improves the estimation of the TC intensification in AROME-IO after 24/30 hr of simulation,
- The OA feedback allowed by the 3D coupling only significantly impact the intensity of slow storms.

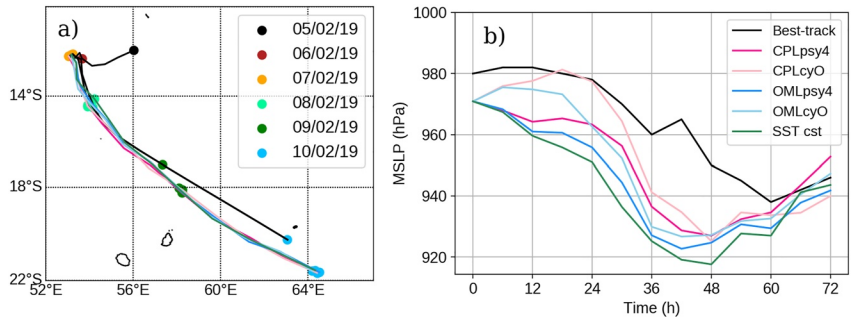

Figure 6. (a) Track of Gelena and (b) time evolution of P_{min} (hPa) for the simulations starting 7 February 2019 at 00 UTC: CPLpsy4 (dark pink line), CPLcyO (light pink line), OMLpsy4 (dark blue line), OMLcyO (light blue line) and SST constant (green line). The BT data (black line) are plotted from 5 February 2019 to 10 February in order to show the quasi-stationarity of the TC the 6 and 7 February 2019.

- The cooling in the oceanic initial conditions that is consistent with the AROME wind forcing only impacts approximately the first 24 hr of the TC intensity forecast when the OML parameterization is later used in the forecast model (OMLcyO).

In the following section, we analyze in more detail the oceanic and the atmospheric responses in the new OA coupled system for three particular cases: TC Gelena from the "slow" group, TC Belna from the "fast" group and TC Batsirai for which we have drifter observations (satellite-tracked drifting buoys).

3.2. Gelena: A Case of Extreme Cooling of the Ocean in AROME-NEMO

3.2.1. Gelena Analysis by the RMSC-La Réunion

Gelena was the ninth tropical storm of the 2018–2019 cyclone season in the SWIO. Gelena formed within an active monsoon trough taking place in early February 2019 over the SWIO from an area of low pressure located less than 1,000 km east of Diego-Suarez (northern tip of Madagascar). It experienced a rapid development late on 5 February 2019 and the system became a TS in the early hours of 6 February. It reached the level of STS, almost TC (equivalent CAT2 on the US Saffir-Simpson scale) at the end of 6 February. It weakened on 7 February due to the cooling of the SST induced by its very slow motion on 6 and 7 February. Gelena accelerated after 7 February and resumed its intensification. It became a TC on the morning of 8 February, then it reached the stage of ITC (equivalent CAT3) 24 hr later. Gelena reached its maximum intensity in the early afternoon of 9 February with maximum winds estimated over 10 min at 57 m s^{-1} (equivalent CAT4) and a minimum sea level pressure of 938 hPa before weakening due to vertical shear. At the end of the night of 9 February, Gelena approached within 60 km of Rodrigues Island as ITC. The island suffered violent wind gusts recorded at 46 m s^{-1} at Pointe-Canon (southeast of Mauricius). During the following days, Gelena moved along a south-east and then east-south-east track and slowly filled in and dissipated at the end of 16 February east of 90°E in the subtropics.

Both the operational models IFS and AROME-IO overestimated the intensity of TC Gelena compared to that estimated by the BT. We hypothesized that the quasi-stationary behavior of Gelena on 6 February and most part of 7 February led to a strong oceanic response which could have been underestimated by the IFS and the current OMLpsy4 configuration of AROME-IO. The comparison of the uncoupled and the coupled simulations which is the subject of the next section confirmed our guess.

3.2.2. Simulations of TC Gelena

In this section, the development of TC Gelena and the corresponding response of the ocean are analyzed with two sets of five runs starting 6 February 2019, 00 UTC and 7 February 2019, 00 UTC.

The TC tracks (Figure 6a) simulated with the CPL (pink curves), OML (blue curves) and SST constant (green line) configurations are similar and close to the BT that is estimated by the RSMC-La Réunion (black line), despite a slight shift to the west after the 8 February 2019, 06 UTC. The mean error (including both along track and across track errors) is approximately 30 km during the first 30 hr of the simulations and it reaches about 200 km at the end of the 72 hr simulations.

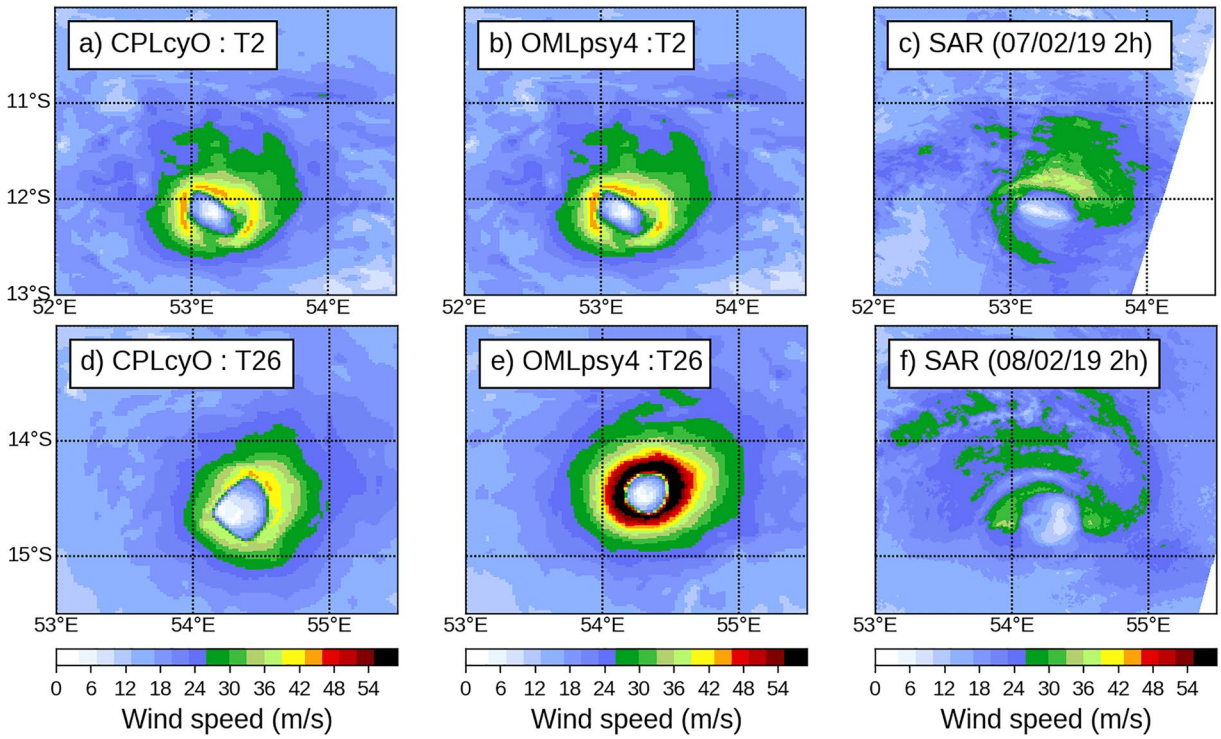

Figure 7. TC Gelena surface winds: (a and b) (resp. d and e) 10 m wind speed (m s^{-1}) of the 2 hr (resp. 26 h) forecasts verifying on 7 February 2019, 02 UTC (resp. 8 February 2019, 02 UTC) for both CPLcyO and OMLpsy4; (c) (resp. f) SAR surface wind speed (m s^{-1}) on 7 February 2019 at 02 UTC (resp. 8 February 2019, 02 UTC).

Gelena has a quasi-stationary behavior on the 6 February 2019 with an average translation speed of 1.5 m s^{-1}. On the 7 February 2019, Gelena maintains a slow translation speed of 3 m s^{-1} and then it accelerates during the next 48 hr, with an average translation speeds of 8 m s^{-1}.

Figure 6b shows the temporal evolution of P_{min} (hPa) derived from the RSMC La Reunion BT data (black), the CPLpsy4 (dark pink), CPLcyO (light pink), OMLpsy4 (dark blue), OMLcyO (lightblue) and SST constant (green) simulations, for the runs starting on the 7 February 2019 at 00 UTC. The impact of cycling the ocean state on the TC intensity is clearly seen on the first 24 hr of the simulations as the psy4 runs are about 10 hPa deeper than the cyO runs. In this case, all runs highly overestimates the intensification after 30 hr of simulation with a simulated maximum of intensity after about 36–48 hr of simulation, 12 hr before the BT. This 12 hr shift is probably due to the remaining tendency of AROME to overestimate the TC intensification when the TC moves away from the strong upwelling. At the peak of intensity, P_{min} in the CPL runs is however about 5 hPa weaker than in the OML runs. The simulation with constant SST (green) shows that neglecting completely the feedback between the TC and the ocean generates in this case an even lager overestimation of maximum TC intensity of about 5 hPa compared to the OMLpsy4 simulation.

Figure 7 shows the surface (10 m) wind speeds of TC Gelena in the run starting on 7 February 2019 for the CPLcyO and OMLpsy4 simulations compared to the SAR data. The surface wind field observed by the SAR shows a maximum wind speed value in the eyewall of 37 m s^{-1} on 7 February 2019 at 02 UTC and about 35 m s^{-1} on the 8 February 2019 at 02 UTC. The winds simulated by the AROME model are much stronger than those observed by the SAR data, especially after 26 hr of simulation with OMLpsy4 when the wind speed values in the eyewall reach about 55–60 m s^{-1}. The maximum wind in CPLcyO is about 15 m s^{-1} weaker, but still more than 10 m s^{-1} higher than the observation.

The response of the ocean to the cyclonic winds in CPLpsy4, CPLcyO, OMLpsy4 and OMLcyO simulations starting on the 7 February 2019 is illustrated in Figures 8–11. In the 3D coupled runs of the 6 February 2019 at 00 UTC (not shown), the cooling of the SST reaches about 6°C in the first 24 hr of the simulations (Figure 8b). Such an intense cooling is not present in the MERCATOR product PSY4 of the 7 February 2019 at 00 UTC (Figure 8a). The initial state of the ocean for the psy4 runs is then about 6°C warmer than the one of the cyO

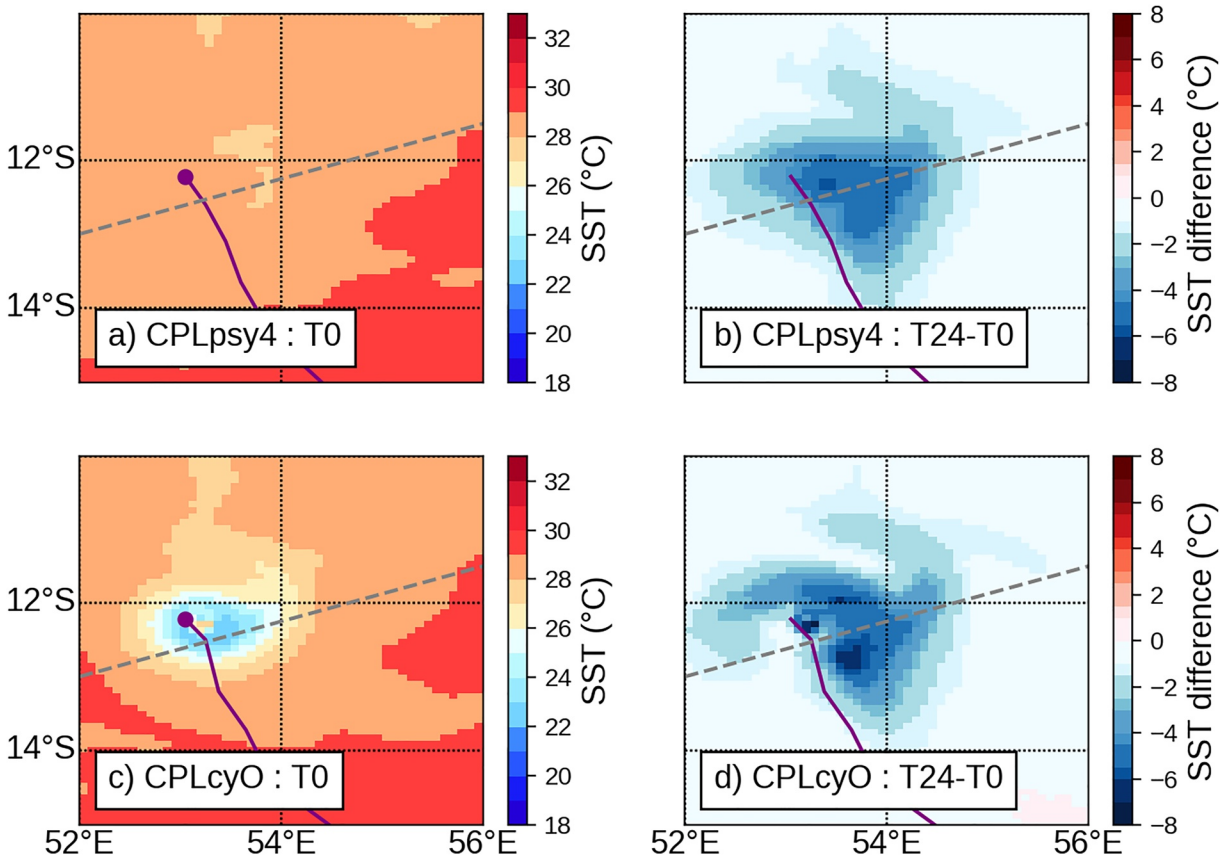

Figure 8. SST (°C) in the vicinity of Gelena for the simulation starting on the 7 February 2019 at 00 UTC: (a–c) initial condition of simulation with the CPLpsy4 (top) and CPLcyO (bottom) configurations and (b–d) SST difference (°C) between the initial condition and the 24 hr forecast. The purple point gives the position of the cyclone at the time of the figure and the track of the cyclone is represented by the purple line.

runs. In both CPL simulations starting 7 February 2019 at 00 UTC, the SST cools by an other 6°C in the first 24 hr of the simulation (Figures 8b–8d) as the TC is still slow. In OMLpsy4, the SST cools only by about 1.5°C (Figure 9b). In the OMLcyO simulation, the SST which had been cooled by 6°C in the previous coupled run now heats up by 2°C (Figure 9d). We will see later in this section that actually, in the first 12 hr of simulation starting on the 7 February 2019, the OA surface fluxes in the CPLcyO and OMLcyO runs tend to heat up the ocean.

This difference in surface water cooling between the CPL and OML simulations is explained by the presence of an intense upwelling in the CPL runs (Figures 10 and 11). In CPLcyO and OMLcyO, the upwelling is already intense in the initial condition of the 7 February 2019 00 UTC (Figures 10 and 11c). It has already crossed the bottom of the OML in the first 24 hr of the previous forecast (CPLcyO from the 6 February 2019 at 00 UTC). In the OMLpsy4 and the CPLpsy4 initial condition, the upwelling is broader and weaker than in cyO runs. It is still confined to about 30 m below the surface (Figure 10a) but the OML has become shallower above the upwelling.

In CPLcyO, the upwelling remains strong in the first 24 hr of the 7 February 2019 00 UTC simulation, cooling the surface by an other 6°C (about twice more than the cooling in the PSY4 products during this period). In CPLpsy4, the upwelling intensifies in the first 24 of simulation such that the SST cools also by about 6°C on 7 February. However, at the end of the quasi-stationary period on 8 February 2019 00 UTC, the surface of the ocean is still 6°C cooler in CPLcyO than in CPLpsy4 because of the SST difference in initial condition.

As expected in the South hemisphere, the upwelling in the CPL runs is located on the left side of the TC track in the direction of propagation (Bielli et al., 2021; Pianezze et al., 2018; Price, 1981), so on the East side of Gelena (Figures 10b–10d). In this zone, the thermocline, which corresponds to the thermal transition zone between the deep cold waters and the warmer well mixed surface waters initially at about 50 m depth, is pushed toward the surface by the upwelling. In the core of the upwelling, the cold water completely replaces the warm waters of

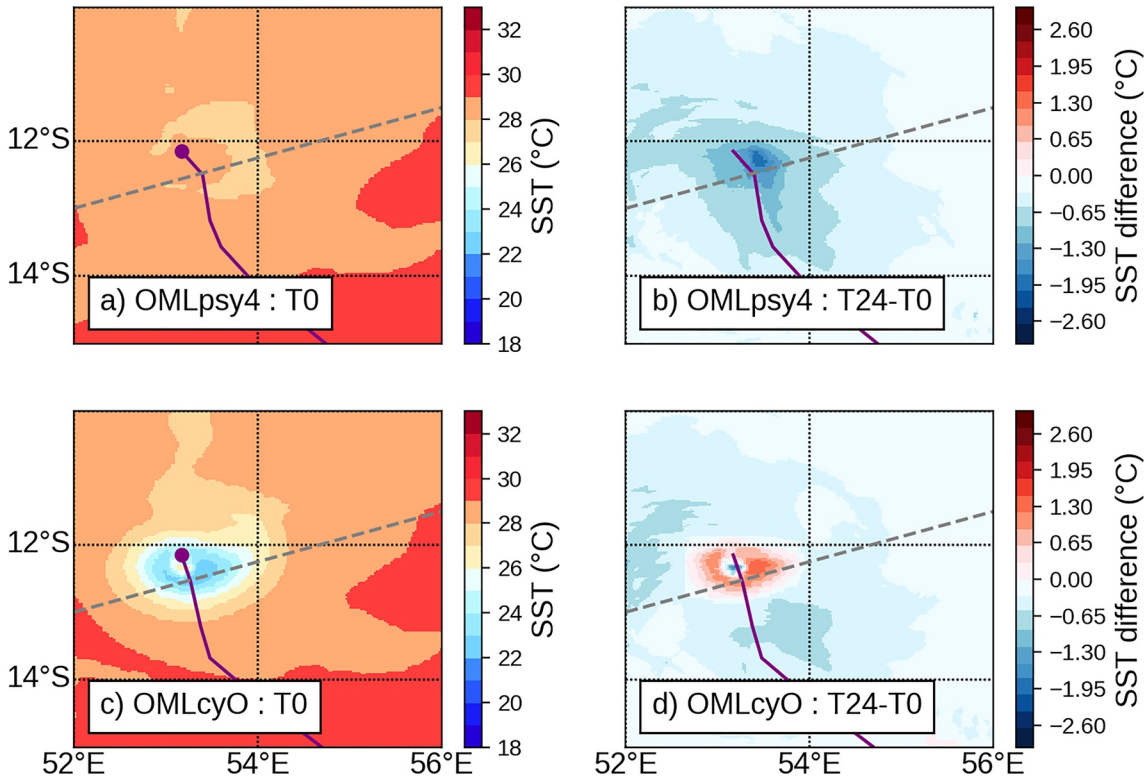

Figure 9. As Figure 8 but for OMLpsy4 and OMLcyO configurations. Note that the color scale for the differences is different for this figure and Figure 8.

the OML to the surface. Also, in both CPL cases, a zone of maximum warming is observed about 2° of longitude on the east side of the TC at a depth between 40 and 80 m. It corresponds to a zone where the turbulent mixing deepens the OML as colder water originally under the initial thermocline is mixed with warmer water from the OML. In this region, the OML deepens.

For the OMLpsy4 simulations (Figure 11), the cooling of the surface waters is very shallow, between the surface and a depth of about 20 m and it does not exceed 2°C. In OMLcyO, the intense upwelling that started in the first 24 hr of the previous is not active in an uncoupled run. It is slowly eroded from the top by the surface fluxes resulting in a weak warming of 1°C in the upper part of the upwelling which was present in the initial condition.

Figure 12 shows the surface latent heat fluxes (W m^{-2}) and the radial and tangential winds (m s^{-1}) at 50 m above the surface around the Gelena center after 6 hr of the simulation starting on the 7 February 2019 at 00 UTC for CPLcyO, CPLpsy4, OMLcyO and OMLpsy4. Both simulations that start with a cycled ocean show a reversal of the heat fluxes at the OA interface of −250 to −500 W m^{-2} meaning that, when the ocean cooling is intense and fast, the atmosphere gives back heat to the ocean contrary to the primary mechanism leading to TC intensification. Such an inversion of sensible and latent heat fluxes between the air and the sea surface is also mentioned by Glenn et al. (2016). The minimum heat flux is observed in the left rear part of the TC track in the region of the strongest upwelling (as shown in Figures 8 and 10). In OMLcyO, the inversion of heat fluxes sign under the TC (Figure 12d) causes a warming of the surface waters which is not compensated by the cooling associated with the turbulent mixing in the OML (Figures 9 and 11).

The processes below and at the surface discussed above have a direct impact on the vertical structure of the TC. Figure 13 illustrates the vertical structure of the mean state of Gelena in its NW and NE quadrants, for the CPLcyO and OMLpsy4 simulations. These two quadrants show the rear area of the cyclone where the cooling was the most intense. In this figure, the intensity of the deep convection is illustrated by synthetic radar reflectivity which are diagnosed in the model. The computation of the synthetic radar reflectivity uses a generic representation of the hydrometeore size distributions. It is implicitly assumed that the radar wavelength is large enough so that radar waves propagate without attenuation and that the Rayleigh scattering approximation is valid (see Richard et al., 2003 for more details). The strong low level convergence simulated by OMLpsy4 results in a

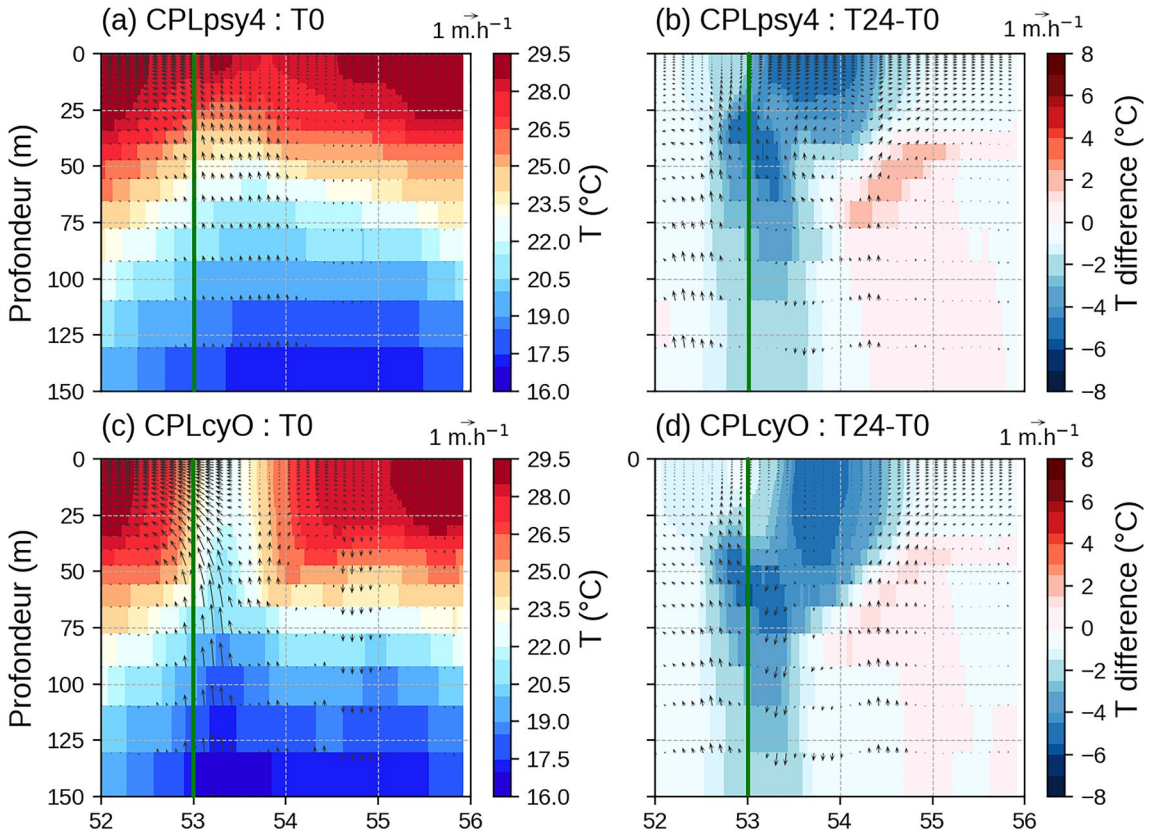

Figure 10. West-East cross-section along the dashed gray line on Figure 8 showing the evolution of the ocean temperature (*T*) in the run starting on the 7 February 2019 at 00 UTC run (a–c) initial condition of simulation with the CPLpsy4 (top) and CPLcyO (bottom) configurations and (b–d) temperature (*T*) difference (°C) between the initial condition and the 24 hr forecast. The green line represents the CT position on 7 February 2019.

strong convective zone, which extends up to 16 km altitude in both quadrants. In this case, the deep convection shows a circular symmetry around the eye. The maximum of synthetic radar reflectivity that is associated with the eyewall extends up to 5 km above the surface. In CPLcyO, the convergent secondary circulation at the surface is weaker. The depth of the deep convection is reduced to 14 km height. In this case, the cyclone is more asymmetric with weaker convection in the NE part above the coldest surface waters. Low level clouds forms in the northern part of the eye where the heat fluxes are negative (Figure 13) while in OMLpsy4, the TC eye remains very dry. Low level clouds in the eye are a well known feature (see e.g., Houze, 2010; Kossin et al., 2002), but to our knowledge, their formation has not yet been linked to the ocean cooling under a TC.

In summary for the case of Gelena, all 5 model configurations overestimate the TC intensity. In the operational configuration OMLpsy4, the maximum wind near the max of intensity is about twice the observed wind speed. The overestimation is reduced by a factor of two in the CPLcyO configuration. The feedback between the upwelling and the TC which is present only in the coupled configurations is a key factor in this case where the TC remains quasi-stationary for almost 48 hr. But, if the coupling with a 3D ocean model partially solves the overestimation of the winds, other components of the model are probably still needed to improve the behavior of the model in the case of intense TC (surface flux parameterization, coupling with waves/sea sprays, currents, cloud microphysics). This case also shows the importance of the choice of oceanic initial condition in short term forecasts. The memory of the oceanic circulations triggered by the high resolution TC winds from AROME is lost if the ocean in the coupled model is initialized by the PSY4 products. The impact on the TC intensity is found to be significant in case of intense cooling.

In the case of Gelena, we could not find any in situ measurements to validate the SST cooling. It is then impossible to conclude on the realism of the 12°C cooling in 48 hr produced by the CPLcyO configuration. References to such large cooling are found in the literature (Chiang et al., 2011; Guan et al., 2021). Our belief is however that

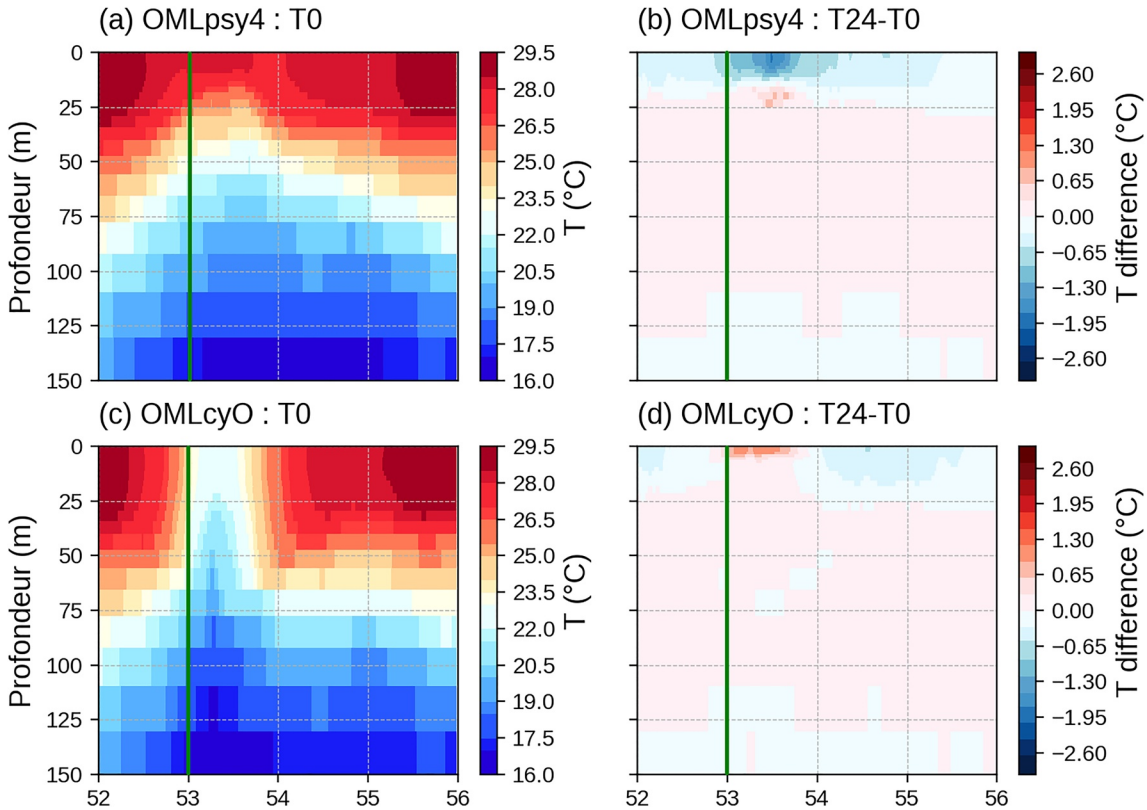

Figure 11. As Figure 10 but for OMLpsy4 and OMLcyO configurations. Note that the color scale for the differences is different for figure and Figure 10.

the ocean cooling that is obtained by the CPLcyO configuration in the case of Gelena is a bit overestimated as a consequence of the overintensification of the TC intensity in AROME-NEMO.

3.3. Belna: A Case of Steadily Moving TC

3.3.1. Belna Analysis by the RMSC-La Réunion

Belna developed within a low level convergence zone resulting from the conjunction of a Madden Julian oscillation phase and the passage of an equatorial Rossby wave in early December 2019 South of the Seychelles. During the night of 05 December, it developed from a moderate to a STS and became a TC on the morning of 07 December. Belna reached its maximum intensity in the late afternoon of 7 December with maximum estimated winds of 43 m s^{-1} and a minimum sea level pressure of 954 hPa. It maintained a south-western track and passed between the islands of Aldabra and Astove and 100 km west of Mayotte during the day on 08 December. It weakened to a STS during the first 6 hr of 09 December, and then re intensified to a TC during the next 6 hr north of Madagascar. During the following days, Belna weakened and it completely dissipated on 11 December.

TC Belna was not moving very fast, but it has a regular pace at about 4 m s^{-1}. It entered the AROME domain during the night of 5 December. We will focus on the run starting on the 6 December 2019 at 00 UTC. In this case, the initial oceanic state from PSY4 and from the cycled ocean configurations are very similar.

3.3.2. Simulations of TC Belna

In this section, the development of TC Belna and the corresponding response of the ocean are analyzed with a set of five runs starting on the 6 December 2019 at 00 UTC.

Figure 14 shows the track of Belna and the time evolution of P_{min} (hPa) as given by the RSMC La Reunion BT data (black) and derived from the CPLpsy4 (dark pink), CPLcyO (light pink), OMLpsy4 (dark blue), OMLcyO (lightblue) and SST constant (green) simulations. As in the case of TC Gelena, Belna tracks are very similar in the five simulations (Figure 14a) and they are close to the BT (black line), with a small westward error in TC position

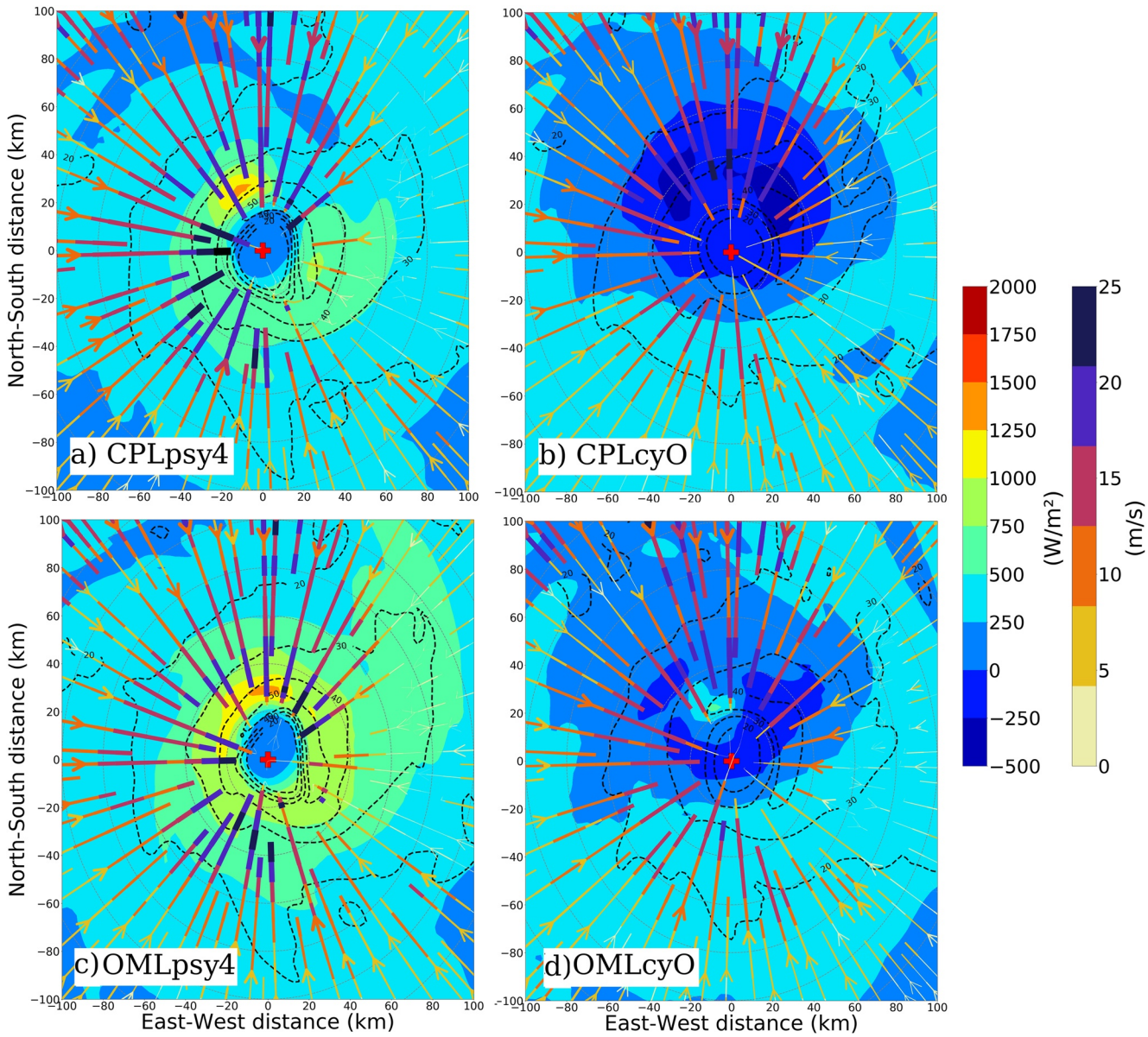

Figure 12. Surface latent heat fluxes (W m^{-2}, shading) near the center of Gelena after 6 hr of simulation of runs starting on the 7 February 2019 at 00 UTC: (a) CPLpsy4, (b) CPLcyO, (c) OMLpsy4 and (d) OMLcyO. The radial wind at 50 m above the surface (m s^{-1}) is represented by the colored arrows and isolines of tangential wind speed (m s^{-1}) are drawn with black dashed contours.

in the first 48 hr of the simulations. The average error is about 60 km over the entire period. The simulated translation speed of Belna is on average 4 m s^{-1} during the whole simulation (not shown). During the first 36 hr, the P_{min} forecast in the 5 configurations remains close to the BT analysis. But after 36 hr, the TC continues to intensify in all model configurations while Belna starts to weaken in the observations.

The anomaly in the forecast is confirmed by the comparison with two SAR images (Figure 15). After 26 hr of simulation, the wind speed values in the eyewall are very similar to those observed on the SAR images, that is, between 30 and 40 m s^{-1}. However, after 50 hr of simulation, a few hours after the intensity peak, the wind speeds in the eyewall are about 30 m s^{-1} higher in the CPLcyO and OMLpsy4 simulations than in the SAR data.

The response of the ocean in CPLcyO and OMLpsy4 simulations starting on the 6 December 2019 is illustrated in Figures 16 and 17. CPLpsy4 (resp. OMLcyO) is not shown because the results are very similar with CPLcyO (resp. OMLpsy4). The CPLcyO and OMLpsy4 simulations start with very similar oceanic states (Figures 16a

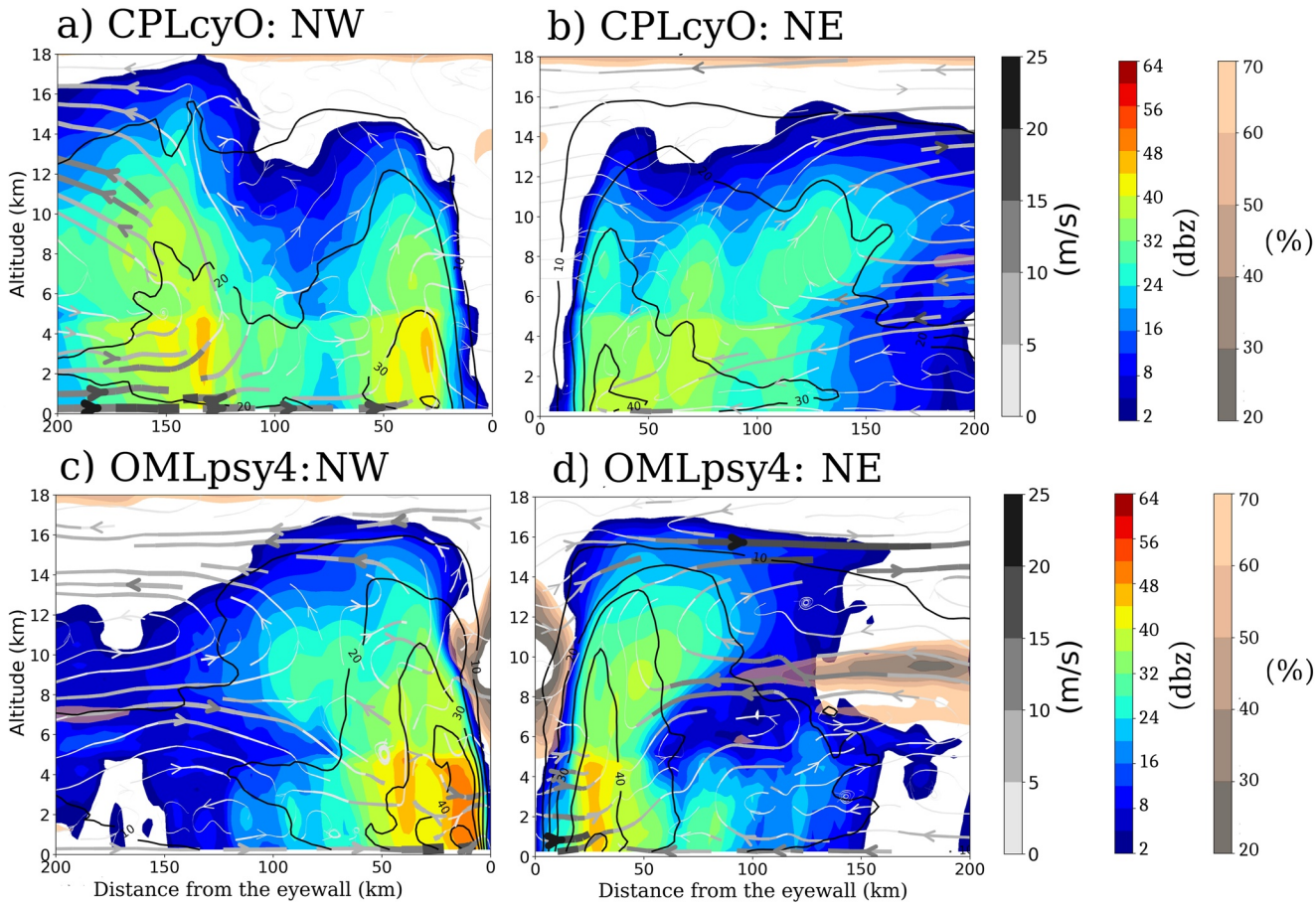

Figure 13. Vertical sections of the azimuthal mean of synthetic radar reflectivity (dBz) for the (a–c) North-West and (b–d) North-East quadrants of Gelena after 12 hr of simulation from the 7 February 2019 at 00 UTC with the OMLpsy4 and CPLcyO configurations. On the same figure, the secondary circulation is shown with streamlines in black and white and the tangential wind speed (m s^{-1}) with black isocontours. Relative humidity (%) is in pink/gray shadings.

and 16c). After 48 hr of simulation, in both CPLcyO and OMLpsy4 the area of SST cooling around the TC is quite large, on both side of the track. The maxima of cooling are however still found on the left (East) side of the track, with a maximum value of 2°C in CPLcyO and OMLpsy4. The vertical cross-section shown in Figure 17 show a narrow upwelling in the CPL run which weaken as it reaches the bottom of the OML. Most of the cold water remains confined under the OML at around 50 m depth. A weak extension of upwelling in the OML may however explain the small difference in SST cooling between the CPLcyO and the OMLpsy4 runs. In this case,

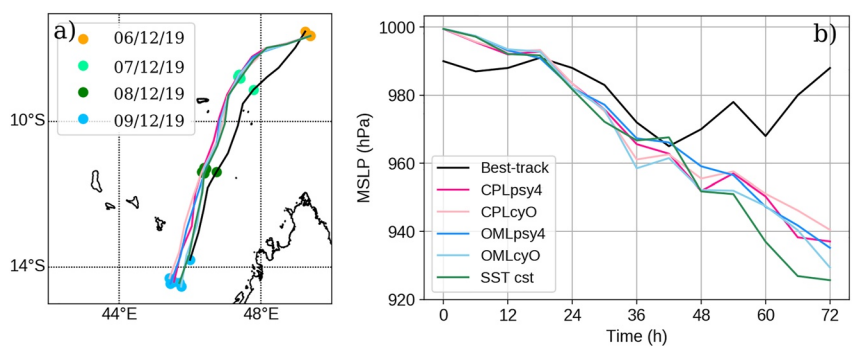

Figure 14. (a) Track of Belna and (b) Time evolution of P_{min} (hPa) from the 06 December 2019 at 00 UTC to the 9 December 2019 at 00 UTC (72 hr) for the RSMC La Réunion BT data (black) and the CPLpsy4 (dark pink), CPLcyO (light pink), OMLpsy4 (dark blue), OMLcyO (light blue) and SST constant (green) configurations.

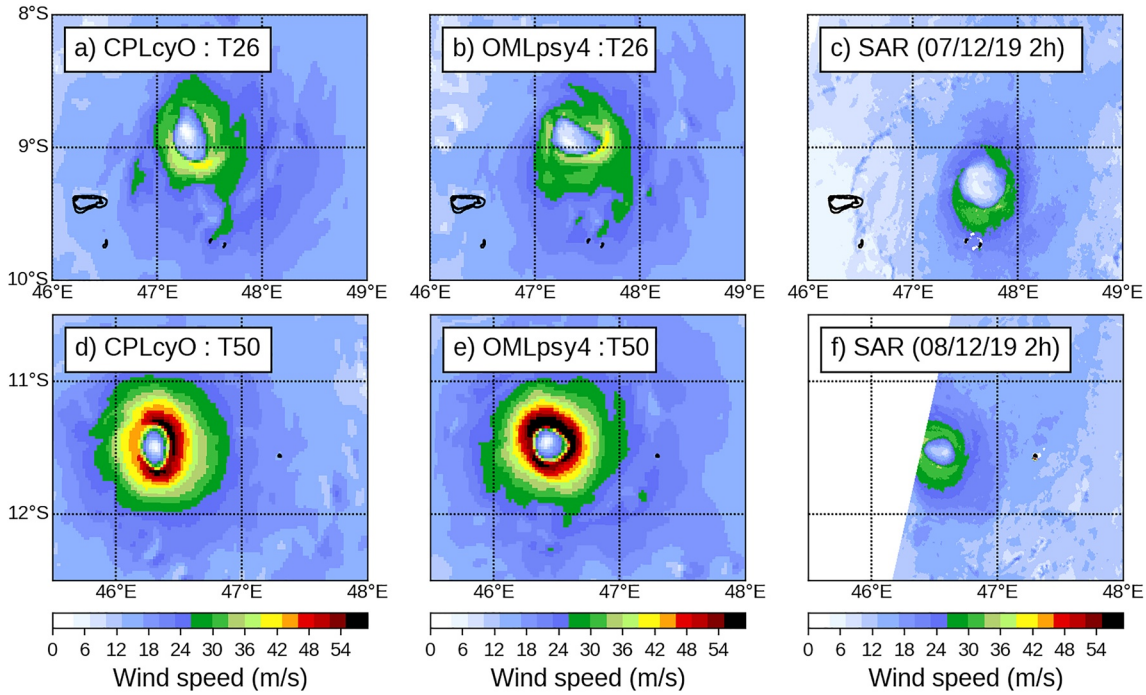

Figure 15. TC Belna surface winds: (a and b) (resp. d and e) 10 m wind speed (m s^{-1}) of the 26 hr (resp. 50 h) forecasts verifying on 7 December 2019, 2 UTC (resp. 8 December 2019, 2 UTC) for both CPLcyO and OMLpsy4; (c) (resp. f) SAR surface wind speed (m s^{-1}) on 7 December 2019 at 2 UTC (resp. 8 December 2019, 2 UTC).

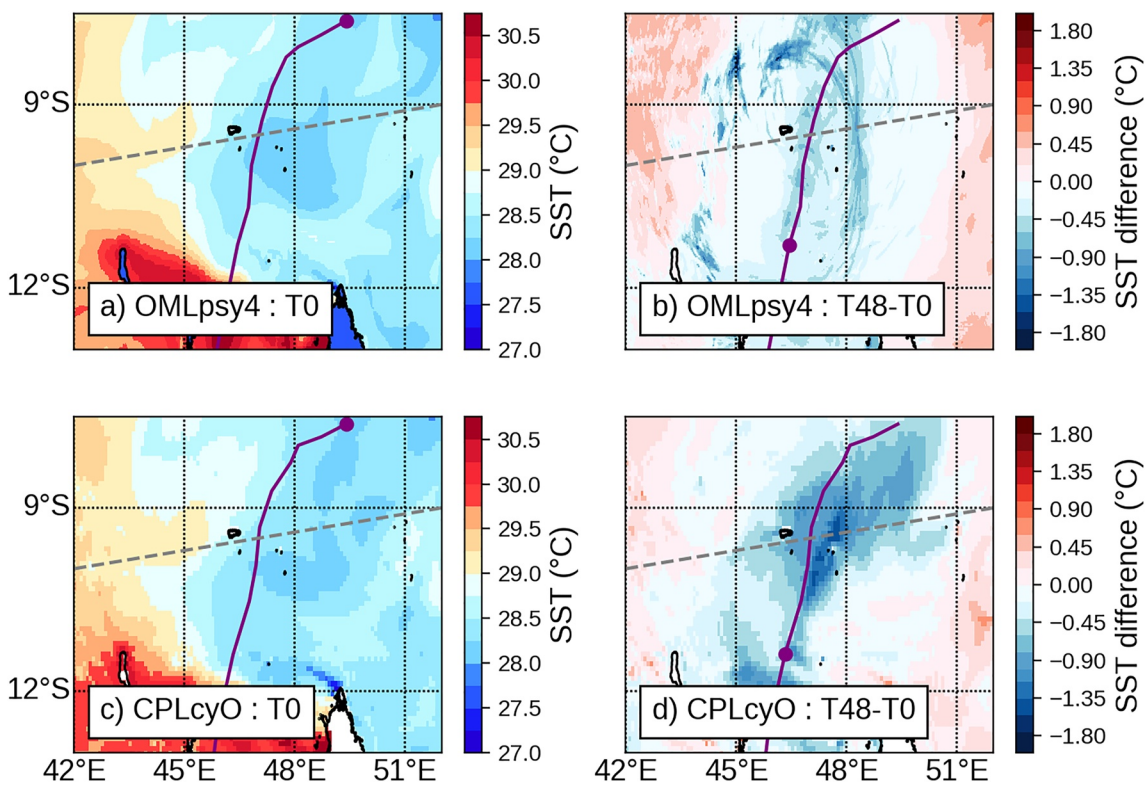

Figure 16. SST (°C) in the vicinity of Belna for the simulation starting at 00 UTC on the 6 December 2019: (a–c) initial condition of simulation with the OMLpsy4 (top) and CPLcyO (bottom) configurations and (b–d) SST difference (°C) between the initial condition and the 48 hr forecast. The purple point gives the position of the cyclone at the time of the figure and the track of the cyclone is represented by the purple line.

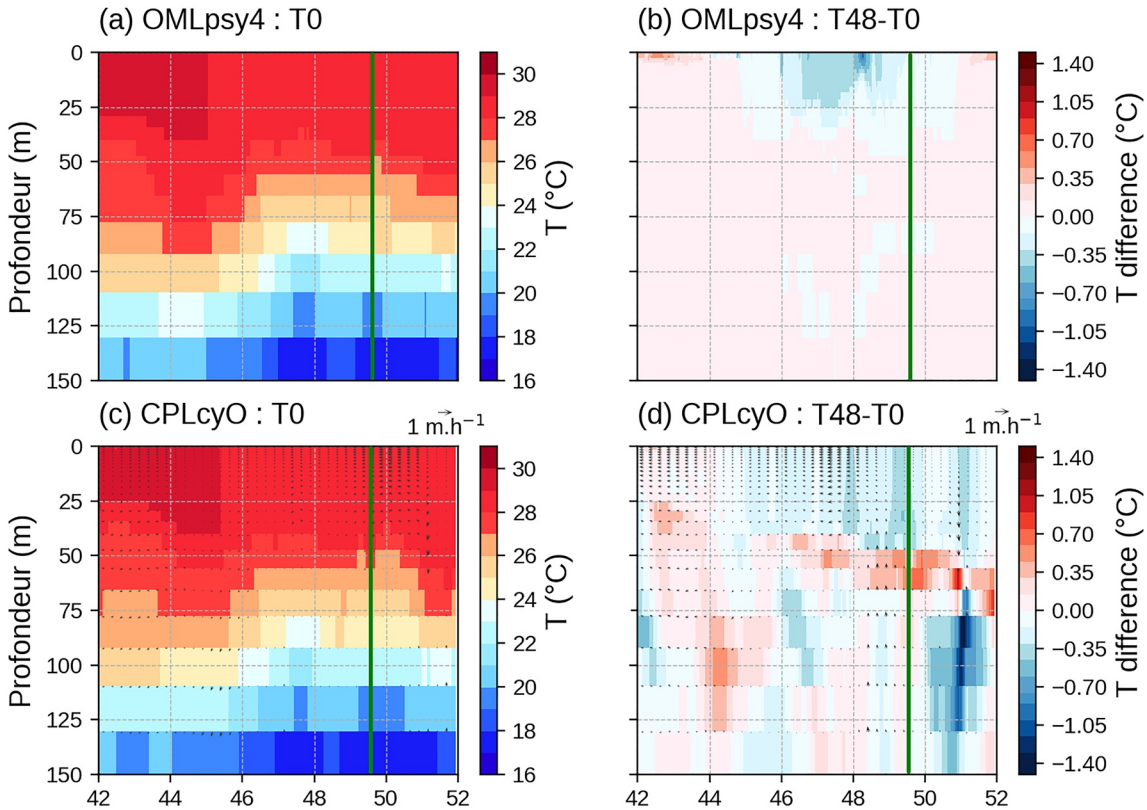

Figure 17. West-East cross-section along the dashed gray line on Figure 16 showing the evolution of the ocean temperature (*T*) in the run of the 6 December 2019 at 00 UTC (a–c) initial condition of simulation with the OMLpsy4 (top) and CPLcyO (bottom) configurations and (b–d) temperature (*T*) difference (°C) between the initial condition and the 48 hr forecast. The vertical green line represents the TC position on 7 February 2019.

the upwelling does not destroy the thermocline, but the depth of the OML becomes deeper below the TC where the turbulent mixing erodes the thermocline as indicated by the positive temperature tendencies between 50 and 70 m in Figure 17d.

In the case of Belna, the impact of the 3D coupling with the ocean is limited. In particular, the lack of coupling was not responsible for the large intensity estimation in the last 36 hr of the operational forecast starting on the 6 December 2019 at 00 UTC. The reason of this intensity error has yet to be understood with future works.

3.4. Batsirai: A Case With Buoy Observations

We present here an analysis of TC Batsirai, which developed into a category 4 TC during the 2021–2022 TC season of the SWIO, and for which in situ buoy observations are available, unlike TCs of the previous three seasons. For this case, we mainly focus on the comparison of the oceanic state of the CPLcyO and OMLpsy4 experiment with the buoy measurements, taking advantage of such a rare opportunity in the SWIO basin to validate the evolution of the SST in the model in the vicinity of a TC with good quality measurements.

3.4.1. Batsirai Analysis by the RMSC-La Réunion

Batsirai was the second tropical system and the first to reach the TC level of the 2021–2022 cyclone season in the SWIO. It formed within a very active monsoon trough on the 24 January 2022 in the northeast of the SWIO basin at the edge of a trans-equatorial monsoon flow. After a short phase of rapid intensification on 27 January, Batsirai weakens over the following days as it encounters larger wind shear and dry air intrusions along its westward track. On 29 January, it meets much more favorable conditions and re-intensifies into a Category 4 hurricane. As it travels north of Mauricius on 31 January, it causes heavy flooding on the Island of St Brandon (northeast of Mauricius) because of the combined effect of a storm surge and a swell with the largest waves estimated between seven and nine m. Batsirai becomes an ITC on 2 February as it is the closest to La Réunion. Winds exceeded

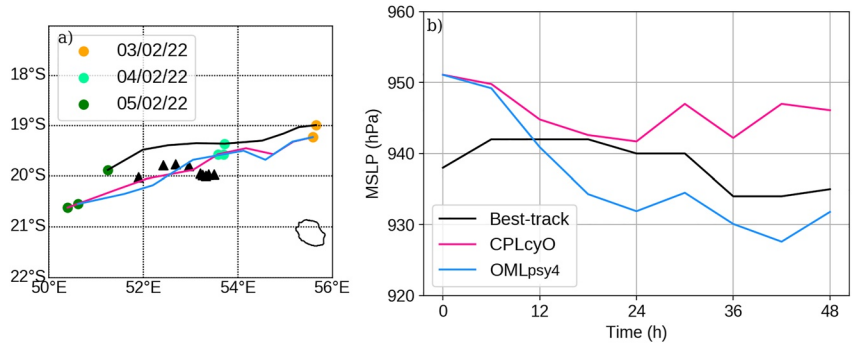

Figure 18. (a) Track of Batsirai and (b) Time evolution of P_{min} (hPa) from the 3 February 2022 at 00 UTC to the 5 February 2022 at 00 UTC (48 hr) for the RSMC La Réunion BT data (black) and the CPLpsy4 (pink) and OMLpsy4 (blue) configurations. The black triangles show the position of a drifting buoy every 6 hr between 3 and 5 February 2022.

42 m s^{-1} in the highest ridges of La Réunion. Exceptional rainfall of about 1,500 mm have been recorded on the volcano area during this episode. The storm underwent an eyewall replacement the following day and fluctuated in intensity before making landfall on the east coast of Madagascar on 5 February as a category 3 cyclone causing at least 121 casualties and a lot of damages on housing and infrastructures. The system then weakened quickly as it crossed Madagascar. It emerged as a TS between Mozambique and southern Madagascar on 7 February, and then became a post-tropical depression on 8 February.

3.4.2. Comparison of TC Batsirai Simulations With Buoy Measurements and SAR Winds

As it is often the case in an operational context, the NWP guidances for TC tracks and intensities are not perfect, but they still remain a valuable source of information for the RSMCs. As Batsirai was at its closest from La Réunion, the uncertainty in the track forecast was still large both in cross track and along track direction in most NWP models. AROME overestimated the speed of displacement and the Southward curvature of Batsirai track. For the more detailed discussion below, we have selected the 48 hr run from the 3 February 2022 at 00 UTC as it covered the period when the TC displacement is the slowest. With the criteria used for the TC of the 2018–2019 and 2019–2020 seasons in the previous sections, Batsirai would be classified as a slow cyclone during this 48 hr period.

The initial intensity of the TC in AROME-IO is underestimated after the 6-hr warmup (Figure 18a). In the operational configuration OMLpsy4 from the 3 February 2022 at 00 UTC, the TC rapidly intensify and overtake the observed intensity after 12 hr of simulation (Figure 18b). In the coupled run CPLcyO, the intensification is weaker (Figure 18) but the winds in the eyewall after 39 hr of simulation are nevertheless 2–3 m s^{-1} stronger than the estimation given by the SAR wind retrieval (Figure 19). At the time of the SAR observation, the asymmetry of the system with weaker winds in the North-East quadrant is better seen in the coupled simulation than in the operational configuration.

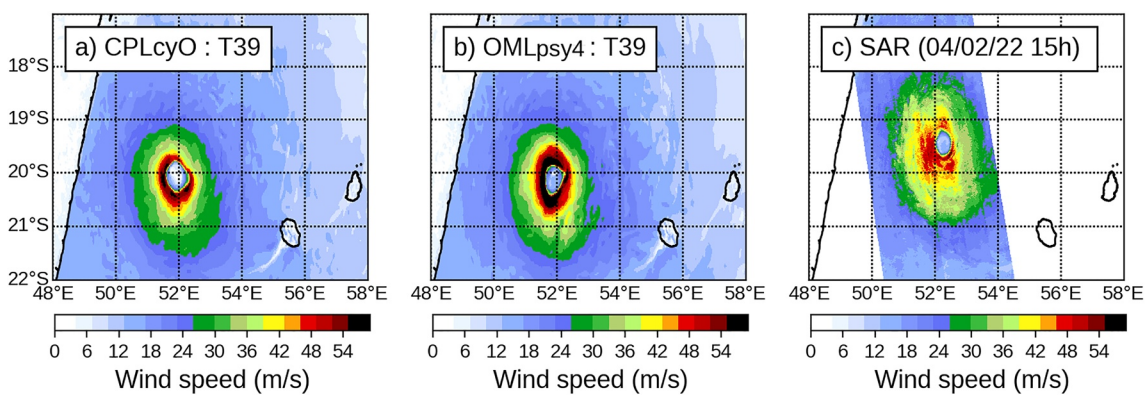

Figure 19. TC Batsirai surface winds: (a and b) 10 m wind speed (m s^{-1}) of the 39 hr forecasts verifying on 4 February 2022, 15 UTC for both CPLcyO and OMLpsy4 (c) SAR surface wind speed (m s^{-1}) on 4 February 2022 at 15 hr.

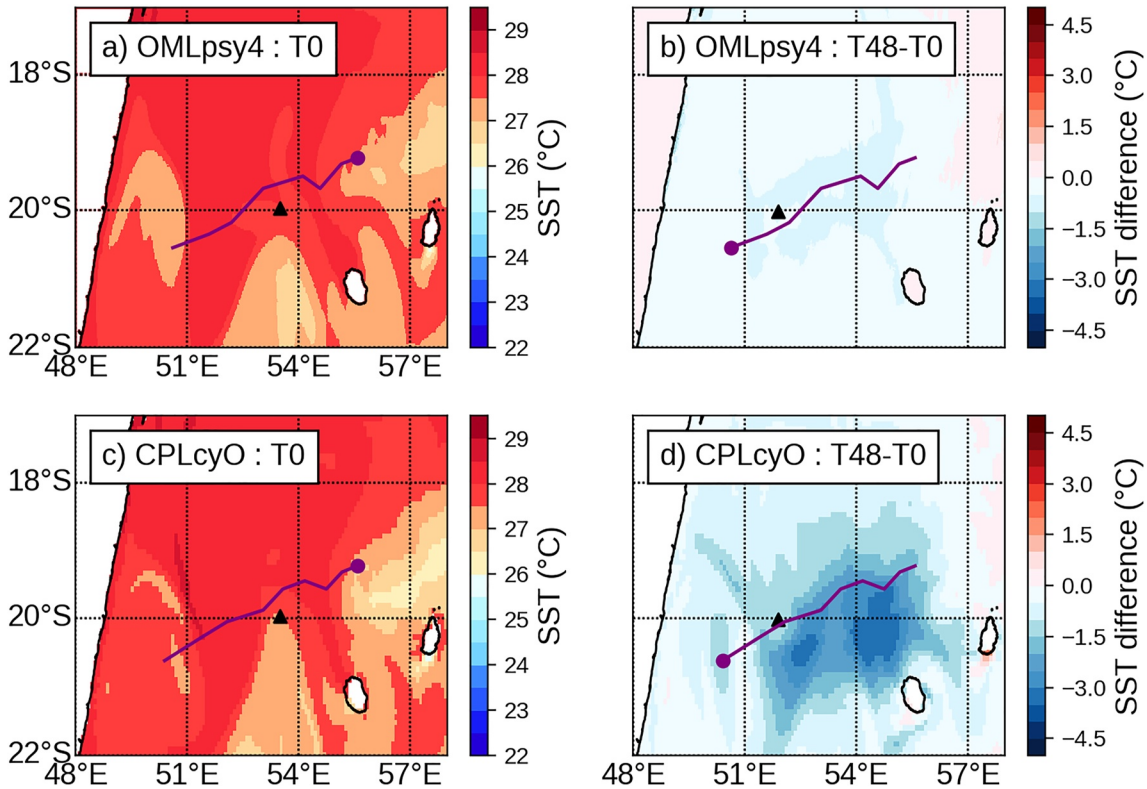

Figure 20. SST (°C) in the vicinity of Batsirai for the simulation starting at 00 UTC on the 3 February 2022: (a–c) initial condition of simulation with the OMLpsy4 (top) and CPLcyO (bottom) configurations and (b–d) SST difference (°C) between the initial condition and the 48 hr forecast. The purple point gives the position of the cyclone at the time of the figure and the track of the cyclone is represented by the purple line. The black triangle show the position of the drifting buoy.

TC Batsirai triggers a SST cooling North of the Mascarene Islands when it displacement velocity is at its slowest. In the cold wake on the South side of Batsirai track simulated by CPLcyO configuration, the maximum cooling is about 4°C (Figure 20). In the OMLpsy4, it is only about 1°C.

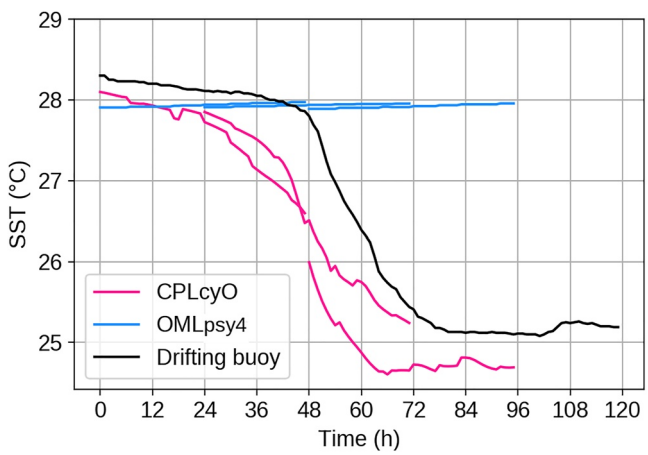

Figure 21. Time evolution of the SST (°C) measured by drifters in the vicinity of Batsirai track (black line). Comparison with SST at the location of the drifters in three successive 48 hr simulations starting on 2–4 February 2022 at 00 UTC, with the CPLcyO configuration (pink) and the OMLpsy4 configuration (blue).

Figure 21 shows the evolution of the SST measured by the drifting buoy indicated by a black triangle on Figure 20 (black line). The SST at the buoy loses about 3°C between the 3 February 2022 at 00 UTC and the 5 February 2022 at 00 UTC. The pink curves on Figure 21 show the evolution of the SST at the position of the buoy in three successive CPLcyO runs (2 February at 00 UTC, 3 February at 00 UTC and 4 February 2022 at 00 UTC). AROME-NEMO reproduces a very similar evolution of the SST but with an advance of about 24 hr. The error in the track position, and especially the along track error that results from an overestimation of the TC translation velocity is a likely reason for the timing error of the SST cooling in the model in this case.

This last case illustrates well the difficulty of the comparison of TC simulations with observations, especially when there is an error in the TC position forecast. However, the confrontation of the buoy observations with the result of the CPLcyO simulation shows that the oceanic response of the coupled system AROME-IO/NEMO is realistic when the surface winds of the TC are close to the observed values.

4. Discussion and Conclusion

The overseas version of the convection-permitting numerical weather prediction model AROME-IO which is used by the RSMC-cyclones of La Réunion,

is coupled every 5 min to a 1D parameterization of the OML. The present study aimed at testing the replacement of the simplified OA interaction described by the 1D parameterization of the OML by a full 3D coupling with the oceanic model NEMO in a future configuration of AROME-IO. The implementation of the coupled configuration AROME-IO/NEMO has been facilitated by former developments which had already been made in the surface platform SURFEX used by AROME. The data exchange between the atmosphere and the ocean is managed by the OASIS coupler. Unlike the 1D parameterization, the ocean model needs boundary conditions which are prepared from the global oceanic products of MERCATOR-Ocean. In the design of the coupled system, we kept in mind the constraints imposed by a future operational system. For example, we only used data sources which would be available in real time. Early on in the design process, the question of the initialization of the ocean has been raised for the case of a forecast system running 4 times a day for short forecasts (48–78 hr). Several solutions have been tested and two of them have been selected for the numerical configurations used in this article.

Atmospheric and oceanic in situ observations in the vicinity of TCs are very sparse in the IO. High resolution satellite wind measurements are irregular and SST products are of low quality due to cloud cover. Unlike in the Atlantic or North Pacific basin, it is difficult to validate NWP configuration against observation. The validation of TC forecast is then often limited to the comparison of macroscopic characteristics such as position, minimum of pressure at the center of the TC and maximum wind. In a few cases, high resolution SAR images and buoys measurement give useful information for model evaluation.

The main results of this study are based on a comparison between five configurations of AROME-IO; one with constant SST, two with the OML parameterization and two with the coupled AROME-NEMO model. For each of these two OA coupling options, the initial condition of the ocean is either directly interpolated from the MERCATOR-Ocean PSY4 products as it is the case for the initialization of the OML in the current operational model or it is cycled by the AROME-NEMO system since a few days before the cyclone intensification. Three-day forecasts for about 30 starting dates and seven different TCs of the 2018–2019 and 2019–2020 TC cyclone seasons have been produced. The simulations are first compared using standard scores against the RSMC BT data. Then, case studies illustrate the differences between the different coupling solution for a selection of 3 TCs.

The scores shows that:

- there is very little impact of the 3D coupling on the TC track. This was expected as, in a limited area model, the track is mainly driven by the larger scale of the host model.
- there is an improvement of the cyclone intensity forecast with the 3D coupling in AROME-IO both in terms of bias and standard deviation. These improvements are particularly true for TCs that encounter a slow propagation phase (less than 2 m s^{-1} for at least 12 hr).
- the memory of the mesoscale OA interaction also contributes to better TC intensity in the first 24–36 hr of the forecast, both for 3D coupling and 1D OML parameterization.

Three case studies confirm that the score improvement is actually due to the better representation of the surface cooling in the vicinity of the TCs when AROME-OI is coupled with NEMO. The vertical advection of deep cold water to the surface which is triggered by the divergence of the surface current is essential, especially for TC with a slow propagation speed (less than 2 m/s) to accurately represent the feedback between the atmosphere and the ocean along the TC track. The detailed analyses of the OA interaction also show that:

- very intense winds in a stationary TC may trigger strong upwelling which are cooling the ocean surface of more than 5°C per day. In such extreme cases, the OA thermodynamic fluxes are reversed compared to the usual TC configuration where the ocean fuels the TCs. The TC intensification is then significantly affected. Intense coolings modify the structure of the boundary layer, both in the wall and in the eye, with possible formation of low level clouds in the eye.
- the 3D upwellings are deep circulations which affect first the bottom of the OML. The strongest upwelling will completely modify the structure of the OML and the well mixed water will be replaced by cold water advected upward across the thermocline. In case of regularly moving TC, weak upwellings are triggered; colder water accumulates under the thermocline and slowly mixes with the upper layer. The feedback on the TC intensity is then weak as the maximum cooling is weaker and anyway, the TC is not affected by the maximum cooling as it has moved on.

Even if the 3D coupling reduces the tendency of AROME-IO to over intensify already intense cyclones, the scores against the BT and the case studies show that the limitation of the simplified 1D coupling with the ocean is only one aspect of the problem as the coupled configurations of the model still overestimates the intensification

for "fast" TCs. One other avenue to explore in order to further improve the TC intensification in the model is to work on the parameterization of the surface fluxes in case of strong winds. There is currently no real consensus about the behavior of the momentum and heat fluxes for very strong winds (and almost no measurements). It may nevertheless be beneficial to move from the strongly parameterize "bulk" scheme ECUME toward a scheme with an explicit representation of the wave drag. We are currently testing the WASP scheme (Wave-Age Stress dependent Parameterization; Sauvage et al., 2020) which has recently been implemented in SURFEX. WASP is based on the COARE3.0 (Fairall et al., 2003) and COARE3.5 (Edson et al., 2013) schemes. It offers the possibility to explicitly account for the wave growth in the calculation of the roughness length at the wind range where the momentum of the atmosphere transferred to the waves is between 7 and 25 m s^{-1}. Above 25 m s^{-1}, the contribution of wave breaking is dominant and the wave age is no longer a sufficient parameter to represent the impact of the sea state on the surface roughness. The contribution of sea sprays to the OA exchanges in case of high winds is also probably to be considered. Several ongoing researches on this topics may contribute to further improvement of the air-sea exchange parameterization in TC conditions. A second avenue of improvement would be to work on the microphysics scheme. The ICE3 microphysics currently used in AROME is a 1 moment microphysics without any direct feedback on aerosol concentration. Tests with a 2 moment microphysics have shown that a prognostic concentration in marine and dust aerosol limits the TC growth (T. Hoarau et al., 2018). However, the introduction of new prognostic variables in the 2 moment microphysics, the cloud condensation nuclei (CCN), brings a new source of uncertainty and should then be very carefully evaluated in the prospective of operational use. In particular, the initialization and the lateral boundary coupling of the aerosol and the parameterization of the sources of aerosol are factors that must be of sufficient quality for the performance of the models to improve.

This study also illustrates the importance of the ocean initial conditions in a coupled NWP suite. We have found that the MERCATOR PSY4 products which are currently forced by winds with a native resolution of about 10 km show a much weaker response in terms of upwelling (but also in term of quasi-inertial waves; G. Hoarau & Malardel, 2021) than what we have found in the coupled AROME-NEMO configuration. Our results show that in a suite where the ocean model is initialized every 24 hr by a new PSY4 ocean state, the fine scale structures which are triggered by the AROME high resolution winds needs to be rebuilt at each model cycle. In this case, the quality of the first 30 hr of forecast, especially for slow or quasi-stationary TCs is degraded compared to a configuration where the initial state of the ocean already contains fine scale structures forced by the AROME winds. We have actually shown that the memory of the high wind forcing can be kept if the ocean state from a previous forecast is used to initialized the next forecast. However, in an operational suite, the ocean cannot be cycled indefinitely without any correction toward oceanic observation. It is then important to implement a solution which combine the PSY4 ocean state which is regularly updated by an oceanic data assimilation and a previous forecast of the ocean which has seen high resolution winds. Several solutions from a simple linear relaxation toward the PSY4 state to more scale selective nudging procedures will be tested.

In this study, we made the choice to use the same atmospheric initial condition for all the experiments in order to focus on the sensitivity to the oceanic component and the coupling solution. But an effort to improve the initial balance between the atmosphere and the ocean in the initial conditions of both fluids will be needed. The simplest solution will be to adapt the warmup procedure which is currently used for the atmosphere to reduce the initial spin-up of the downscaling adjustment of the IFS fields to the AROME resolution to the coupled configuration. In parallel, research and development activities toward a coupled data assimilation system for AROME are starting in the research groups at Météo-France.

AROME-NEMO is an evolution toward a more realistic regional forecast system for TCs. With a resolution of 1/12 of a degree and a coupling frequency of 1 hr, the computational cost of the ocean model NEMO remains negligible compared to the cost of the atmospheric model AROME. There is however a clear increase in the complexity of the forecast suite as the suite needs to prepare the initial and lateral boundary conditions for NEMO and the data to feed the OASIS coupler at the beginning of the simulation. If this configuration was meant to become operational with 4 runs a day, technical work would be needed in order to automate the processing of the NEMO initial and lateral boundary condition files in real time.

Different tests are still on going in order to check the sensitivity to vertical and horizontal resolution of the ocean (for a given atmospheric resolution), the coupling frequency and other specific options of NEMO such as the barometric effect which may be of interest for the surge forecast at the coast associated with TC landing. However, a fine representation of coastal effects requires an increase toward kilometric horizontal resolution in

the ocean and an upgrade in complexity of the model in order to include new processes such as tides, river run off. This would significantly increase the computer cost of the coupled configuration. Such options will first be tested in research mode before being tested, in a distant future, for operational applications.

Finally, the new suite would need to be tested for a long and continuous period during a full TC season, but also during the dry season. The use of specific scores (Ebert, 2008; Roberts & Lean, 2008), more adapted to extreme phenomena such as TC and to fine scale numerical forecasts, should make it possible to further validate the coupled configuration in terms of atmospheric parameters, cloud structures and precipitation.

Data Availability Statement

The atmospheric model used in this study is AROME Cycle 43t2 which has been the operational version of the AROME-overseas from July 2019 to June 2022. AROME is available for non-commercial research purpose upon signature of a license agreement, see http://www.accord-nwp.org/?ACCORD-MoU-2021-2025. The ocean model is NEMO, version 3.6, which can be downloaded at https://www.nemo-ocean.eu. All the material which is necessary to reproduce the numerical simulations has been published on zenodo.org with the https://doi.org/10.5281/zenodo.7241990. The SAR data have been uploaded from https://cyclobs.ifremer.fr/app/ and the data from the ARGO drifters from http://www.coriolis.eu.org/Data-Products/Data-selection. The Best Track data have been extracted from the Best Track database of the Direction Régional de l'Océan Indien (DIROI) of Météo-France. These data are shared with the IBTracs database (https://www.ncdc.noaa.gov/ibtracs/) after a subjective reanalysis by the DIROI forecasters at the end of each TC season.

Acknowledgments
This work was supported by a PhD Grant from Météo-France. We thank Ségolène Berthou and an anonymous reviewer for their very interesting and constructive comments.

References

Amante, C., & Eakins, B. W. (2009). ETOPO1 global relief model converted to PanMap layer format [Dataset]. PANGAEA. https://doi.org/10.1594/PANGAEA.769615

Andreas, E. L., Mahrt, L., & Vickers, D. (2015). An improved bulk air–sea surface flux algorithm, including spray-mediated transfer. *Quarterly Journal of the Royal Meteorological Society*, *141*(687), 642–654. https://doi.org/10.1002/qj.2424

Bao, J., Wilczak, J., Choi, J., & Kantha, L. (2000). Numerical simulations of air–sea interaction under high wind conditions using a coupled model: A study of hurricane development. *Monthly Weather Review*, *128*(7), 2190–2210. https://doi.org/10.1175/1520-0493(2000)128<2190:nsoasi>2.0.co;2

Belamari, S. (2005). Report on uncertainty estimates of an optimal bulk formulation for surface turbulent fluxes. *Marine EnviRonment and Security for the European Area–Integrated Project (MERSEA IP), Deliverable D*, *4*, 505.

Bender, M. A., Ginis, I., & Kurihara, Y. (1993). Numerical simulations of tropical cyclone-ocean interaction with a high-resolution coupled model. *Journal of Geophysical Research*, *98*(D12), 23245–23263. https://doi.org/10.1029/93jd02370

Bender, M. A., Ginis, I., Tuleya, R., Thomas, B., & Marchok, T. (2007). The operational GFDL coupled hurricane–ocean prediction system and a summary of its performance. *Monthly Weather Review*, *135*(12), 3965–3989. https://doi.org/10.1175/2007mwr2032.1

Bidlot, J. R. (2022). Air sea exchange and wind wave interactions. Retrieved from https://events.ecmwf.int/event/300/contributions/3266/attachments/1924/3469/AS2022_Bidlot.pdf

Bielli, S., Barthe, C., Bousquet, O., Tulet, P., & Pianezze, J. (2021). The effect of atmosphere–ocean coupling on the structure and intensity of tropical cyclone Bejisa in the Southwest Indian Ocean. *Atmosphere*, *12*(6), 688. https://doi.org/10.3390/atmos12060688

Black, P. G. (1983). *Ocean temperature changes induced by tropical cyclones*. The Pennsylvania State University.

Bloom, S., Takacs, L., Da Silva, A., & Ledvina, D. (1996). Data assimilation using incremental analysis updates. *Monthly Weather Review*, *124*(6), 1256–1271. https://doi.org/10.1175/1520-0493(1996)124<1256:dauiau>2.0.co;2

Bougeault, P., & Lacarrere, P. (1989). Parameterization of orography-induced turbulence in a mesobeta–scale model. *Monthly Weather Review*, *117*(8), 1872–1890. https://doi.org/10.1175/1520-0493(1989)117<1872:pooiti>2.0.co;2

Bousquet, O., Barbary, D., Bielli, S., Kebir, S., Raynaud, L., Malardel, S., & Faure, G. (2020). An evaluation of tropical cyclone forecast in the Southwest Indian Ocean basin with AROME-Indian Ocean convection-permitting numerical weather predicting system. *Atmospheric Science Letters*, *21*(3), e950. https://doi.org/10.1002/asl.950

Bousquet, O., Barruol, G., Cordier, E., Barthe, C., Bielli, S., Calmer, R., et al. (2021). Impact of tropical cyclones on inhabited areas of the SWIO Basin at present and future horizons. Part 1: Overview and observing component of the research project renovrisk-cyclone. *Atmosphere*, *12*(5), 544. https://doi.org/10.3390/atmos12050544

Browne, P., de Rosnay, P., & Zuo, H. (2019). Coupled ocean–atmosphere data assimilation at ECMWF. *ECMWF Newsletter*, *160*, 23–28. https://doi.org/10.21957/ka471pbj9e

Castillo, J. M., Lewis, H. W., Mishra, A., Mitra, A., Polton, J., Brereton, A., et al. (2022). The Regional Coupled Suite (RCS-IND1): Application of a flexible regional coupled modelling framework to the Indian region at kilometre scale. *Geoscientific Model Development*, *15*(10), 4193–4223. https://doi.org/10.5194/gmd-15-4193-2022

Chang, S. W., & Anthes, R. A. (1978). Numerical simulations of the ocean's nonlinear, baroclinic response to translating hurricanes. *Journal of Physical Oceanography*, *8*(3), 468–480. https://doi.org/10.1175/1520-0485(1978)008<0468:nsoton>2.0.co;2

Chiang, T.-L., Wu, C.-R., & Oey, L.-Y. (2011). Typhoon Kai-Tak: An ocean's perfect storm. *Journal of Physical Oceanography*, *41*(1), 221–233. https://doi.org/10.1175/2010jpo4518.1

Courtney, J. B., Langlade, S., Barlow, S., Birchard, T., Knaff, J. A., Kotal, S., et al. (2019). Operational perspectives on tropical cyclone intensity change Part 2: Forecasts by operational agencies. *Tropical Cyclone Research and Review*, *8*(4), 226–239. https://doi.org/10.1016/j.tcrr.2020.01.003

Craig, A., Valcke, S., & Coquart, L. (2017). Development and performance of a new version of the OASIS coupler, OASIS3-MCT_3.0. *Geoscientific Model Development*, *10*(9), 3297–3308. https://doi.org/10.5194/gmd-10-3297-2017

Duong, Q.-P., Langlade, S., Payan, C., Husson, R., Mouche, A., & Malardel, S. (2021). C-band SAR winds for tropical cyclone monitoring and forecast in the South-West Indian Ocean. *Atmosphere*, *12*(5), 576. https://doi.org/10.3390/atmos12050576

Dvorak, V. (1975). Tropical cyclone intensity analysis and forecasting from satellite imagery. *Monthly Weather Review*, *103*(5), 420–430. https://doi.org/10.1175/1520-0493(1975)103<0420:tciaaf>2.0.co;2

Dvorak, V. (1984). Tropical cyclone intensity analysis using satellite data. *NOAA Technical Report* (Vol. *11*).

Ebert, E. E. (2008). Fuzzy verification of high-resolution gridded forecasts: A review and proposed framework. *Meteorological Applications*, *15*(1), 51–64. https://doi.org/10.1002/met.25

Edson, J. B., Jampana, V., Weller, R. A., Bigorre, S. P., Plueddemann, A. J., Fairall, C. W., et al. (2013). On the exchange of momentum over the open ocean. *Journal of Physical Oceanography*, *43*(8), 1589–1610. https://doi.org/10.1175/JPO-D-12-0173.1

Fairall, C. W., Bradley, E. F., Hare, J. E., Grachev, A. A., & Edson, J. B. (2003). Bulk parameterization of air–sea fluxes: Updates and verification for the COARE algorithm. *Journal of Climate*, *16*(4), 571–591. https://doi.org/10.1175/1520-0442(2003)016⟨0571:BPOASF⟩2.0.CO;2

Faure, G., Chambon, P., & Brousseau, P. (2020). Operational implementation of the AROME model in the tropics: Multiscale validation of rainfall forecasts. *Weather and Forecasting*, *35*(2), 691–710. https://doi.org/10.1175/waf-d-19-0204.1

Feng, X., Klingaman, N. P., & Hodges, K. I. (2019). The effect of atmosphere–ocean coupling on the prediction of 2016 western North Pacific tropical cyclones. *Quarterly Journal of the Royal Meteorological Society*, *145*(723), 2425–2444. https://doi.org/10.1002/qj.3571

Gaspar, P., Grégoris, Y., & Lefevre, J.-M. (1990). A simple eddy kinetic energy model for simulations of the oceanic vertical mixing: Tests at station Papa and Long-Term Upper Ocean Study site. *Journal of Geophysical Research*, *95*(C9), 16179–16193. https://doi.org/10.1029/jc095ic09p16179

Ginis, I. (2002). Tropical cyclone-ocean interactions. *Advances in Fluid Mechanics*, *33*, 83–114.

Glenn, S., Miles, T., Seroka, G., Xu, Y., Forney, R., Yu, F., et al. (2016). Stratified coastal ocean interactions with tropical cyclones. *Nature Communications*, *7*(1), 1–10. https://doi.org/10.1038/ncomms10887

Guan, S., Zhao, W., Sun, L., Zhou, C., Liu, Z., Hong, X., et al. (2021). Tropical cyclone-induced sea surface cooling over the Yellow Sea and Bohai Sea in the 2019 Pacific typhoon season. *Journal of Marine Systems*, *217*, 103509. https://doi.org/10.1016/j.jmarsys.2021.103509

Haiden, T., Janousek, M., Bidlot, J., Buizza, R., Ferranti, L., Prates, F., & Vitart, F. (2018). *Evaluation of ECMWF forecasts, including the 2018 upgrade*. European Centre for Medium Range Weather Forecasts.

Heming, J. T., Prates, F., Bender, M. A., Bowyer, R., Cangialosi, J., Caroff, P., et al. (2019). Review of recent progress in tropical cyclone track forecasting and expression of uncertainties. *Tropical Cyclone Research and Review*, *8*(4), 181–218. https://doi.org/10.1016/j.tcrr.2020.01.001

Hermes, J. C., & Reason, C. J. (2009). The sensitivity of the Seychelles–Chagos thermocline ridge to large-scale wind anomalies. *ICES Journal of Marine Science*, *66*(7), 1455–1466. https://doi.org/10.1093/icesjms/fsp074

Hoarau, G., & Malardel, S. (2021). Oceanic evaluation of the AROME-NEMO coupled system by ALAMO float measurements: Case of cyclone FLORENCE (Technical Report). Retrieved from https://www.umr-cnrm.fr/IMG/pdf/r_r_2021-en_web.pdf

Hoarau, T., Barthe, C., Tulet, P., Claeys, M., Pinty, J., Bousquet, O., et al. (2018). Impact of the generation and activation of sea salt aerosols on the evolution of Tropical Cyclone Dumile. *Journal of Geophysical Research: Atmospheres*, *123*(16), 8813–8831. https://doi.org/10.1029/2017jd028125

Houze, R. A. (2010). Clouds in tropical cyclones. *Monthly Weather Review*, *138*(2), 293–344. https://doi.org/10.1175/2009mwr2989.1

Janssen, P., Doyle, J. D., Bidlot, J., Hansen, B., Isaksen, L., & Viterbo, P. (2002). Impact and feedback of ocean waves on the atmosphere. *Advances in Fluid Mechanics*, *33*, 155–198.

Jullien, S., Marchesiello, P., Menkes, C. E., Lefèvre, J., Jourdain, N. C., Samson, G., & Lengaigne, M. (2014). Ocean feedback to tropical cyclones: Climatology and processes. *Climate Dynamics*, *43*(9–10), 2831–2854. https://doi.org/10.1007/s00382-014-2096-6

Jullien, S., Menkès, C. E., Marchesiello, P., Jourdain, N. C., Lengaigne, M., Koch-Larrouy, A., et al. (2012). Impact of tropical cyclones on the heat budget of the South Pacific Ocean. *Journal of Physical Oceanography*, *42*(11), 1882–1906. https://doi.org/10.1175/jpo-d-11-0133.1

Kossin, J. P., McNoldy, B. D., & Schubert, W. H. (2002). Vortical swirls in hurricane eye clouds. *Monthly Weather Review*, *130*(12), 3144–3149. https://doi.org/10.1175/1520-0493(2002)130⟨3144:VSIHEC⟩2.0.CO;2

Lebeaupin Brossier, C., Ducrocq, V., & Giordani, H. (2009). Two-way one-dimensional high-resolution air–sea coupled modelling applied to Mediterranean heavy rain events. *Quarterly Journal of the Royal Meteorological Society: A Journal of the Atmospheric Sciences, Applied Meteorology and Physical Oceanography*, *135*(638), 187–204. https://doi.org/10.1002/qj.338

Lellouche, J.-M., Greiner, E., Le Galloudec, O., Garric, G., Regnier, C., Drevillon, M., et al. (2018). Recent updates to the Copernicus Marine Service global ocean monitoring and forecasting real-time 1/12° high-resolution system. *Ocean Science*, *14*(5), 1093–1126. https://doi.org/10.5194/os-14-1093-2018

Lemarié, F. (2015). *Numerical modification of atmospheric models to include the feedback of oceanic currents on air-sea fluxes in ocean-atmosphere coupled models* (Unpublished doctoral dissertation). INRIA Grenoble-Rhône-Alpes; Laboratoire Jean Kuntzmann; Universite de Grenoble.

Leroux, M.-D., Meister, J., Mekies, D., Dorla, A.-L., & Caroff, P. (2018). A climatology of southwest Indian Ocean tropical systems: Their number, tracks, impacts, sizes, empirical maximum potential intensity, and intensity changes. *Journal of Applied Meteorology and Climatology*, *57*(4), 1021–1041. https://doi.org/10.1175/jamc-d-17-0094.1

Lin, I., Wu, C.-C., Pun, I.-F., & Ko, D.-S. (2008). Upper-ocean thermal structure and the western North Pacific category 5 typhoons. Part I: Ocean features and the category 5 typhoons' intensification. *Monthly Weather Review*, *136*(9), 3288–3306. https://doi.org/10.1175/2008mwr2277.1

Madec, G., Bourdallé-Badie, R., Chanut, J., Clementi, E., Coward, A., Ethé, C., et al. (2019). NEMO ocean engine [Dataset]. Zenodo. https://doi.org/10.5281/zenodo.3878122

Madec, G., Delecluse, P., Imbard, M., & Lévy, C. (1998). OPA 8.1 Ocean General Circulation Model reference manual. *Note du Pôle de modélisation* (Vol. *11*, p. 91).

Madec, G., & Imbard, M. (1996). A global ocean mesh to overcome the north pole singularity. *Climate Dynamics*, *12*(6), 381–388. https://doi.org/10.1007/bf00211684

Magnusson, L., Bidlot, J.-R., Bonavita, M., Brown, A., Browne, P., De Chiara, G., et al. (2019). ECMWF activities for improved hurricane forecasts. *Bulletin of the American Meteorological Society*, *100*(3), 445–458. https://doi.org/10.1175/bams-d-18-0044.1

Mogensen, K. S., Magnusson, L., & Bidlot, J.-R. (2017). Tropical cyclone sensitivity to ocean coupling in the ECMWF coupled model. *Journal of Geophysical Research: Oceans*, *122*(5), 4392–4412. https://doi.org/10.1002/2017jc012753

Moon, I.-J., Ginis, I., & Hara, T. (2004). Effect of surface waves on air–sea momentum exchange. Part II: Behavior of drag coefficient under tropical cyclones. *Journal of the Atmospheric Sciences*, *61*(19), 2334–2348. https://doi.org/10.1175/1520-0469(2004)061<2334:eoswoa>2.0.co;2

Mouche, A. A., Chapron, B., Zhang, B., & Husson, R. (2017). Combined co-and cross-polarized SAR measurements under extreme wind conditions. *IEEE Transactions on Geoscience and Remote Sensing*, *55*(12), 6746–6755. https://doi.org/10.1109/tgrs.2017.2732508

Penny, S. G., Akella, S., Alves, O., Bishop, C., Buehner, M., Chevallier, M., et al. (2017). *Coupled data assimilation for integrated earth system analysis and prediction: Goals, challenges and recommendations (Technical Report)*. World Meteorological Organization. Retrieved from https://library.wmo.int/doc_num.php?explnum_id=10830

Pianezze, J., Barthe, C., Bielli, S., Tulet, P., Jullien, S., Cambon, G., et al. (2018). A new coupled ocean-waves-atmosphere model designed for tropical storm studies: Example of tropical cyclone Bejisa (2013–2014) in the South-West Indian Ocean. *Journal of Advances in Modeling Earth Systems*, *10*(3), 801–825. https://doi.org/10.1002/2017ms001177

Pineau-Guillou, L., Ardhuin, F., Bouin, M.-N., Redelsperger, J.-L., Chapron, B., Bidlot, J.-R., & Quilfen, Y. (2018). Strong winds in a coupled wave–atmosphere model during a North Atlantic storm event: Evaluation against observations. *Quarterly Journal of the Royal Meteorological Society*, *144*(711), 317–332. https://doi.org/10.1002/qj.3205

Price, J. F. (1981). Upper ocean response to a hurricane. *Journal of Physical Oceanography*, *11*(2), 153–175. https://doi.org/10.1175/1520-0485(1981)011<0153:uortah>2.0.co;2

Renault, L., Lemarié, F., & Arsouze, T. (2019). On the implementation and consequences of the oceanic currents feedback in ocean–atmosphere coupled models. *Ocean Modelling*, *141*, 101423. https://doi.org/10.1016/j.ocemod.2019.101423

Richard, E., Cosma, S., Tabary, P., Pinty, J.-P., & Hagen, M. (2003). High-resolution numerical simulations of the convective system observed in the Lago Maggiore area on 17 September 1999 (MAP IOP 2a). *Quarterly Journal of the Royal Meteorological Society: A Journal of the Atmospheric Sciences, Applied Meteorology and Physical Oceanography*, *129*(588), 543–563. https://doi.org/10.1256/qj.02.50

Roberts, N. M., & Lean, H. W. (2008). Scale-selective verification of rainfall accumulations from high-resolution forecasts of convective events. *Monthly Weather Review*, *136*(1), 78–97. https://doi.org/10.1175/2007mwr2123.1

Sauvage, C., Lebeaupin Brossier, C., Bouin, M.-N., & Ducrocq, V. (2020). Characterization of the air–sea exchange mechanisms during a Mediterranean heavy precipitation event using realistic sea state modelling. *Atmospheric Chemistry and Physics*, *20*(3), 1675–1699. https://doi.org/10.5194/acp-20-1675-2020

Schade, L. R., & Emanuel, K. A. (1999). The ocean's effect on the intensity of tropical cyclones: Results from a simple coupled atmosphere–ocean model. *Journal of the Atmospheric Sciences*, *56*(4), 642–651. https://doi.org/10.1175/1520-0469(1999)056<0642:toseot>2.0.co;2

Seity, Y., Brousseau, P., Malardel, S., Hello, G., Bénard, P., Bouttier, F., et al. (2011). The AROME-France convective-scale operational model. *Monthly Weather Review*, *139*(3), 976–991. https://doi.org/10.1175/2010mwr3425.1

Shpund, J., Khain, A., & Rosenfeld, D. (2019). Effects of sea spray on the dynamics and microphysics of an idealized tropical cyclone. *Journal of the Atmospheric Sciences*, *76*(8), 2213–2234. https://doi.org/10.1175/jas-d-18-0270.1

Srinivas, C., Mohan, G. M., Naidu, C., Baskaran, R., & Venkatraman, B. (2016). Impact of air-sea coupling on the simulation of tropical cyclones in the North Indian Ocean using a simple 3-D ocean model coupled to ARW. *Journal of Geophysical Research: Atmospheres*, *121*(16), 9400–9421. https://doi.org/10.1002/2015jd024431

Vellinga, M., Copsey, D., Graham, T., Milton, S., & Johns, T. (2020). Evaluating benefits of two-way ocean–atmosphere coupling for global NWP forecasts. *Weather and Forecasting*, *35*(5), 2127–2144. https://doi.org/10.1175/waf-d-20-0035.1

Vialard, J., Foltz, G., Mcphaden, M. J., Duvel, J.-P., & de Boyer Montégut, C. (2008). Strong Indian Ocean sea surface temperature signals associated with the Madden-Julian Oscillation in late 2007 and early 2008. *Geophysical Research Letters*, *35*(19), L19608. https://doi.org/10.1029/2008gl035238

Vincent, E. M., Lengaigne, M., Madec, G., Vialard, J., Samson, G., Jourdain, N., et al. (2012). Processes setting the characteristics of sea surface cooling induced by tropical cyclones. *Journal of Geophysical Research*, *117*(C2), C02020. https://doi.org/10.1029/2011jc007396

Voldoire, A., Decharme, B., Pianezze, J., Lebeaupin Brossier, C., Sevault, F., Seyfried, L., et al. (2017). SURFEX v8.0 interface with OASIS3-MCT to couple atmosphere with hydrology, ocean, waves and sea-ice models, from coastal to global scales. *Geoscientific Model Development*, *10*(11), 4207–4227. https://doi.org/10.5194/gmd-10-4207-2017

Weill, A., Eymard, L., Caniaux, G., Hauser, D., Planton, S., Dupuis, H., et al. (2003). Toward a better determination of turbulent air–sea fluxes from several experiments. *Journal of Climate*, *16*(4), 600–618. https://doi.org/10.1175/1520-0442(2003)016<0600:tabdot>2.0.co;2

Yablonsky, R. M. (2016). Ocean component of the HWRF coupled model and model evaluation. In *Advanced numerical modeling and data assimilation techniques for tropical cyclone prediction* (pp. 267–304). Springer.

Yablonsky, R. M., & Ginis, I. (2009). Limitation of one-dimensional ocean models for coupled hurricane–ocean model forecasts. *Monthly Weather Review*, *137*(12), 4410–4419. https://doi.org/10.1175/2009mwr2863.1